

# Series system reliability of uncertain linear structures under Gaussian excitation by cross entropy-based importance sampling

Oindrila Kanjilal<sup>1</sup>, Iason Papaioannou<sup>2</sup>, and Daniel Straub<sup>3</sup>

<sup>1</sup>Post-doctoral Fellow, Engineering Risk Analysis Group, Technische Universität München, München 80290, Germany. Email: oindrila.kanjilal@tum.de. Corresponding author

<sup>2</sup>Senior Researcher, Engineering Risk Analysis Group, Technische Universität München, München 80290, Germany. Email: iason.papaioannou@tum.de

<sup>3</sup>Associate Professor, Engineering Risk Analysis Group, Technische Universität München, München 80290, Germany. Email: straub@tum.de

## ABSTRACT

We present an adaptive importance sampling (IS) method to estimate the reliability of linear structures with parameter uncertainties that are subjected to Gaussian process excitation. Structural failure is defined as a union of multiple first-passage failure events. The main contribution is the introduction of an efficient IS density for the uncertain structural parameters. This density is determined by minimizing the cross entropy (CE) between the theoretically optimal IS density of the structural parameters and a chosen parametric family of probability distributions. The CE minimization procedure requires evaluation of the system failure probability conditional on fixed values of the uncertain parameters. A closed-form analytical approximation of this conditional failure probability is derived based on an upper bound on the out-crossing rate. Finally, a joint IS density of the random excitation and the uncertain structural parameters is introduced to estimate the series system failure probability involving parameter uncertainties. The accuracy and efficiency of the proposed method is demonstrated by means of two examples: the first involves a Gaussian white noise-excited two-story linear shear frame and the second involves a six-story three-bay moment resisting steel frame subjected to a filtered non-stationary Gaussian excitation.

## INTRODUCTION

Structural reliability analysis aims at computing the probability of failure of a structure with respect to a prescribed failure criterion by accounting for the uncertainties in the structural parameters (the geometric and material properties) and the external loading. When the load is dynamic, such as the one arising from earthquakes, wind or sea waves, the reliability is estimated in terms of the first-passage probability, i.e., the probability that the dynamic response of the structure exceeds a prescribed threshold level over the duration of the excitation. In general, reliability analysis is usually classified into two categories: component reliability, which considers only a single mode of failure, and system reliability, in which multiple failure modes are considered. This paper focuses on the estimation of series system reliability of uncertain linear structures subjected to Gaussian process excitation. Here the system failure event is defined as the union of first-passage events associated with multiple critical responses.

The series system reliability cannot be directly deduced from the marginal first-passage probabilities of the output responses if the component failure events are statistically dependent. Such dependence is usually present when the component first-passage events occur due a common source of excitation or when the resistances of the components are dependent. For the case where the structural parameters are deterministic and the applied excitation is modeled as a Gaussian process, there are several approaches to estimate the series system reliability. Analytical approximations of the failure probability based on the joint out-crossing rate of Gaussian responses processes are proposed in (Li and Melchers 1993; Song and Der Kiureghian 2006). Bounds can be obtained on the system reliability using analytical bounding formulas (Melchers and Beck 2018) or linear programming (Song and Der Kiureghian 2003; Byun and Song 2020). Alternatively, the Monte Carlo simulation (MCS) method can be applied to estimate the system failure probability. This approach is devoid of assumptions (Poisson assumption for the number of out-crossings) and, hence, is asymptotically exact with increase in the number of samples. The main challenge in applying MCS lies in controlling the sampling variance of the failure probability estimator; the aim is to obtain probability estimates of acceptable accuracy with a small number of dynamic model

52 runs. Reduction in sampling variance is achieved by advanced Monte Carlo methods such as subset  
53 simulation (Au and Beck 2001a), Girsanov's transformation-based IS (Kanjilal and Manohar 2019)  
54 and line sampling (Koutsourelakis et al. 2004; Schuëller et al. 2004b). Efficient simulation meth-  
55 ods that are specific to deterministic linear dynamical systems have also been developed. These  
56 methods increase the efficiency of estimation by utilizing the linearity of the structural response  
57 with respect to the Gaussian loading. The central theme of these methods is to express the failure  
58 region of the series system in terms of a large number of linear failure regions corresponding to  
59 the failure of a particular output response at a particular time instant. In (Au and Beck 2001b) this  
60 strategy is applied to design an effective IS density of the random excitation. Other approaches to  
61 estimate the system reliability based on this concept are studied in (Katafygiotis and Cheung 2004;  
62 Katafygiotis and Cheung 2006; Misraji et al. 2020).

63 When the structural parameters are uncertain and the excitation is a Gaussian random process,  
64 the response is non-linear with respect to the structural parameters. In this case, estimation of the  
65 series system reliability becomes considerably more involved. The MCS method is the most viable  
66 approach to tackle this class of problems. The subset simulation method can be readily applied  
67 to this case. Alternatively, efforts to extend the tailored approaches for Gaussian process-excited  
68 deterministic linear systems to deal with structural parameter uncertainties have been attempted in  
69 (Jensen and Valdebenito 2007; Pradlwarter and Schuëller 2010; Valdebenito et al. 2014). In these  
70 studies, the system failure probability conditional on a given realization of the uncertain parameters  
71 is determined using the approach in (Au and Beck 2001b). The unconditional failure probability  
72 of the series system is then estimated by integrating the conditional probability over the domain of  
73 the uncertain parameters by importance sampling (Jensen and Valdebenito 2007; Valdebenito et al.  
74 2014) or line sampling (Pradlwarter and Schuëller 2010). These methods require system specific  
75 information to facilitate reliability estimation. In (Jensen and Valdebenito 2007; Pradlwarter and  
76 Schuëller 2010), a pseudo-design point with respect to the uncertain structural parameters has to be  
77 identified. These approaches can be effective when there is a unique design point (in the parameter  
78 space) contributing to the failure probability. The IS method in (Valdebenito et al. 2014) makes

79 use of a surrogate model for the probability of failure as a function of the uncertain parameters.  
80 The performance of the method thus relies on the proper choice of the surrogate model, which is  
81 not a straightforward task when the number of uncertain parameters is large or the dependence of  
82 the conditional failure probability on the parameters is strongly non-linear.

83 The present contribution develops an adaptive importance sampling method to estimate the  
84 series system reliability of uncertain linear structures subjected to Gaussian loading. It is an ex-  
85 tension of a recently developed method for component-level first-passage probability estimation  
86 of structures with parameter uncertainty (Kanjilal et al. 2021). The proposed approach employs  
87 the strategy presented in (Au and Beck 2001b) to construct a conditional (on a fixed value of  
88 the structural parameters) IS density of the random loading. A novel IS density of the uncertain  
89 structural parameters is then introduced. This IS density is obtained through application of the  
90 cross entropy (CE) method. The CE method is an adaptive sampling approach that determines  
91 a near-optimal IS density through minimizing the Kullback-Leibler (KL) divergence between the  
92 theoretically optimal IS density and a chosen parametric family of probability distributions. We  
93 discuss appropriate distribution models for the chosen parametric family, depending on the dimen-  
94 sion of parameter uncertainties and the number of failure modes. The CE optimization requires  
95 evaluation of the system failure probability conditional on sample realizations of the uncertain  
96 parameters. To ensure smooth convergence to the optimal IS density, we employ an analytical ap-  
97 proximation of the conditional failure probability during optimization. The approximation is based  
98 on an upper bound on the joint out-crossing rate of the critical responses (Li and Melchers 1993).  
99 In this study, we derive a closed-form analytical solution of the upper bound, which enables faster  
100 evaluation of the conditional probability during CE optimization. Finally, a joint IS density of the  
101 uncertain structures and the random excitation is considered to estimate the failure probability of  
102 the series system. Unlike the methods in (Jensen and Valdebenito 2007; Pradlwarter and Schuëller  
103 2010; Valdebenito et al. 2014), the proposed approach is completely adaptive and can be used as a  
104 black-box algorithm as it does not require problem-specific adjustments. It is therefore more robust  
105 and generally applicable to any linear dynamical system.

## PROBLEM FORMULATION

### Linear Dynamical System

We consider an  $n$  degree-of-freedom linear structure with uncertain parameters subjected to non-stationary stochastic excitation. The governing equation describing the response of the structure is expressed as

$$\mathbf{M}(\boldsymbol{\Theta})\ddot{\mathbf{X}}(t) + \mathbf{C}(\boldsymbol{\Theta})\dot{\mathbf{X}}(t) + \mathbf{K}(\boldsymbol{\Theta})\mathbf{X}(t) = \mathbf{D}\mathbf{f}(t), \quad (1)$$

where  $\ddot{\mathbf{X}}$ ,  $\dot{\mathbf{X}}$  and  $\mathbf{X}$  are the  $n \times 1$  acceleration, velocity and displacement vectors,  $\mathbf{M}$ ,  $\mathbf{C}$  and  $\mathbf{K}$  are the  $n \times n$  mass, damping and stiffness matrices,  $\boldsymbol{\Theta}$  is an  $n_{\theta} \times 1$  vector of random variables that model the uncertain structural parameters,  $\mathbf{f}$  is an  $l \times 1$  vector of random dynamic loads acting on the structure over a time span  $t \in [0, T]$  and  $\mathbf{D}$  is an  $n \times l$  matrix that couples the external excitation with the degrees of freedom of the structure. We consider the case where the components of  $\mathbf{f}$  are Gaussian random processes.

Let  $\{Z_i; i = 1, \dots, m\}$  be  $m$  critical output responses. In a linear system, the relationship between the input excitation and the output response is linear, and can be written as

$$Z_i(t, \boldsymbol{\theta}) = \sum_{j=1}^l \int_0^t K_{ij}(t - \tau; \boldsymbol{\theta}) f_j(\tau) d\tau = \int_0^t \mathbf{K}_i^T(t - \tau; \boldsymbol{\theta}) \mathbf{f}(\tau) d\tau. \quad (2)$$

In the above equation,  $\boldsymbol{\theta}$  denotes a particular outcome of the uncertain structural parameter vector  $\boldsymbol{\Theta}$  and  $K_{ij}(t; \boldsymbol{\theta})$  denotes the unit impulse response function for the  $i$ -th output at time  $t$  due to a unit impulse applied at the  $j$ -th input at time  $t = 0$ , where the outputs are assumed to start from zero initial conditions without loss of generality. Consider a discrete time representation of the time interval  $[0, T]$ . Let  $\{t_k = (k - 1)\Delta t; k = 1, \dots, n_T\}$  be the time instants of analysis, where  $n_T$  is the number of time points and  $\Delta t = T/(n_T - 1)$  is the time step size. Let  $\mathbf{f}(t_k)$  denote the stochastic excitation at time  $t = t_k$ . For Gaussian loading, one can represent  $\mathbf{f}(t_k)$  by a linear combination of an  $n_g \times 1$  standard Gaussian random vector  $\boldsymbol{\Xi}$  as  $\mathbf{f}(t_k) = \mathbf{G}_k \boldsymbol{\Xi}$ , where  $\{\mathbf{G}_k, k = 1, \dots, n_T\}$  are appropriate deterministic matrices. Then the discrete-time analog of the input-output relationship

130 in Eq. (2) is given by

$$131 \quad Z_i(t_k, \boldsymbol{\theta}, \boldsymbol{\Xi}) = \sum_{s=1}^k c_s \mathbf{K}_i^T(t_k - t_s; \boldsymbol{\theta}) \mathbf{f}(t_s) \Delta t = \mathbf{r}_{i,k}^T(\boldsymbol{\theta}) \boldsymbol{\Xi}, \quad (3)$$

132 where  $\mathbf{r}_{i,k}^T(\boldsymbol{\theta}) = \sum_{s=1}^k c_s \mathbf{K}_i^T(t_k - t_s; \boldsymbol{\theta}) \mathbf{G}_s \Delta t$  and  $c_s$  is a coefficient that depends on the particular  
133 numerical integration scheme used to integrate Eq. (2).

### 134 Series System Reliability

135 Reliability analysis of dynamical systems involves the computation of the first-passage proba-  
136 bility. In a series system defined in terms of  $m$  output responses, first-passage failure occurs when  
137 any one of the outputs  $\{Z_i, i = 1, \dots, m\}$  exceeds a corresponding threshold level  $z_i^*$  within the  
138 time duration  $T$ . The system level failure event  $F$  is therefore expressed as

$$139 \quad F = \bigcup_{i=1}^m F_i, \quad (4)$$

140 where

$$141 \quad F_i = \left\{ \boldsymbol{\theta} \in \mathbb{R}^{n_\theta}, \boldsymbol{\xi} \in \mathbb{R}^{n_\xi} : \max_{k=1, \dots, n_T} |Z_i(t_k, \boldsymbol{\theta}, \boldsymbol{\xi})| \geq z_i^* \right\} \quad (5)$$

142 denotes first-passage failure with respect to the  $i$ -th output response. The probability of occurrence  
143 of  $F$  can be expressed by means of the multi-dimensional integral

$$144 \quad P_F = \int_{\boldsymbol{\theta} \in \mathbb{R}^{n_\theta}} P_{F|\boldsymbol{\Theta}}(\boldsymbol{\theta}) p_{\boldsymbol{\Theta}}(\boldsymbol{\theta}) d\boldsymbol{\theta}, \quad (6)$$

145 where

$$146 \quad P_{F|\boldsymbol{\Theta}}(\boldsymbol{\theta}) = \int_{\boldsymbol{\xi} \in \mathbb{R}^{n_\xi}} \mathbf{I}\{(\boldsymbol{\theta}, \boldsymbol{\xi}) \in F\} p_{\boldsymbol{\Xi}}(\boldsymbol{\xi}) d\boldsymbol{\xi} \quad (7)$$

147 represents the conditional probability of failure of the system given the uncertain parameters  $\boldsymbol{\theta}$ . In  
148 the above equations,  $p_{\boldsymbol{\Xi}}(\boldsymbol{\xi})$  and  $p_{\boldsymbol{\Theta}}(\boldsymbol{\theta})$ , respectively, denote the joint probability density function  
149 (PDF) of  $\boldsymbol{\Xi}$  and  $\boldsymbol{\Theta}$ , and  $\mathbf{I}\{(\boldsymbol{\theta}, \boldsymbol{\xi}) \in F\}$  is the indicator function for the failure event which takes the

150 value 1 if  $(\boldsymbol{\theta}, \boldsymbol{\xi}) \in F$  and is 0 otherwise.

151 A convenient way to evaluate  $P_F$  is by Monte Carlo simulation (MCS). In principle, one could  
152 use the standard Monte Carlo method. When the probability of failure is small, standard MCS  
153 requires a very large number of dynamical system evaluations to generate accurate results. In this  
154 paper we develop an alternative strategy based on importance sampling (IS) to estimate the series  
155 system reliability. To this end, we note that the study in (Au and Beck 2001b) introduces an IS  
156 density of the random vector  $\boldsymbol{\Xi}$  modeling the dynamic load, which enables efficient estimation of the  
157 conditional probability of failure  $P_{F|\boldsymbol{\Theta}}(\boldsymbol{\theta})$  by IS. Therefore, the key challenge in the construction of  
158 an efficient IS estimator for  $P_F$  lies in the design of an effective IS density to integrate  $P_{F|\boldsymbol{\Theta}}(\boldsymbol{\theta})$  over  
159 the domain of the uncertain parameter vector  $\boldsymbol{\Theta}$ . In the next section, we present a novel approach to  
160 determine this IS density using the cross entropy method. Subsequently, we combine the proposed  
161 IS density of  $\boldsymbol{\Theta}$  with the IS density of  $\boldsymbol{\Xi}$  to obtain the estimator for the first-passage probability of  
162 the series system.

## 163 DETERMINATION OF THE IS DENSITY OF $\boldsymbol{\Theta}$

164 Evaluation of the dynamic system reliability of uncertain structures according to Eq. (6) requires  
165 integration of the conditional failure probability  $P_{F|\boldsymbol{\Theta}}(\boldsymbol{\theta})$  over the sample space of  $\boldsymbol{\Theta}$ . In order to  
166 evaluate the integral by IS, an IS density  $h_{\boldsymbol{\Theta}}(\boldsymbol{\theta})$  of the structural parameters is introduced. The  
167 integral in Eq. (6) is modified to

$$168 P_F = \int_{\boldsymbol{\theta} \in \mathbb{R}^{n_{\boldsymbol{\theta}}}} P_{F|\boldsymbol{\Theta}}(\boldsymbol{\theta}) W(\boldsymbol{\theta}) h_{\boldsymbol{\Theta}}(\boldsymbol{\theta}) d\boldsymbol{\theta}, \quad (8)$$

169 where  $W(\boldsymbol{\theta}) = p_{\boldsymbol{\Theta}}(\boldsymbol{\theta})/h_{\boldsymbol{\Theta}}(\boldsymbol{\theta})$  is the importance weight function. Based on Eq. (8), one can  
170 estimate  $P_F$  using the following IS estimator:

$$171 \hat{P}_F = \frac{1}{N_R} \sum_{i=1}^{N_R} P_{F|\boldsymbol{\Theta}}(\boldsymbol{\theta}^{(i)}) W(\boldsymbol{\theta}^{(i)}), \quad (9)$$

172 where  $\{\boldsymbol{\theta}^{(i)}; i = 1, \dots, N_R\}$  are independent samples distributed according to  $h_{\boldsymbol{\Theta}}(\boldsymbol{\theta})$ . The coef-

173 ficient of variation (CoV) of the IS estimator depends on the choice of  $h_{\Theta}(\theta)$ . The theoretically  
 174 optimal IS density that leads to an estimator with zero variance is given by

$$175 \quad h_{\Theta}^*(\theta) = \frac{1}{P_F} P_{F|\Theta}(\theta) p_{\Theta}(\theta). \quad (10)$$

176 In practice, it is not possible to sample from this IS density since  $P_F$  is not known. Instead, we  
 177 construct an IS density for  $\Theta$  that is a close approximation of  $h_{\Theta}^*(\theta)$  using the cross entropy (CE)  
 178 method.

179 The CE method is an adaptive approach to determine a near-optimal IS density through mini-  
 180 mizing the Kullback-Leibler (KL) divergence between the theoretically optimal IS density  $h_{\Theta}^*(\theta)$   
 181 and a chosen parametric family of probability distributions. Let  $h_{\Theta}(\theta; \nu)$  be a family of para-  
 182 metric densities, where  $\nu \in \mathcal{V}$  is the parameter vector, such that it contains the nominal density,  
 183  $p_{\Theta}(\theta)$ , of the uncertain parameters. The KL divergence between  $h_{\Theta}^*(\theta)$  and  $h_{\Theta}(\theta; \nu)$  is defined  
 184 as (Rubinstein and Kroese 2016)

$$185 \quad D(h_{\Theta}^*(\theta), h_{\Theta}(\theta; \nu)) = E_{h_{\Theta}^*} \left[ \ln \left( \frac{h_{\Theta}^*(\theta)}{h_{\Theta}(\theta; \nu)} \right) \right]. \quad (11)$$

186 The basic idea of the CE method is to determine the optimal parameter vector  $\nu^*$  that minimizes  
 187  $D(h_{\Theta}^*(\theta), h_{\Theta}(\theta; \nu))$ . Substitution of the expression of  $h_{\Theta}^*(\theta)$  in Eq. (10) into Eq. (11) yields the  
 188 following CE optimization problem:

$$189 \quad \nu^* = \operatorname{argmax}_{q \in \mathcal{V}} E_{p_{\Theta}} [P_{F|\Theta}(\theta) \ln (h_{\Theta}(\theta; q))]. \quad (12)$$

190 The above optimization can be solved by approximating the expectation in Eq. (12) using a set of  
 191 samples distributed according to  $p_{\Theta}(\theta)$ . However, in practical applications, the optimal density  
 192  $h_{\Theta}^*(\theta)$  can differ significantly from  $p_{\Theta}(\theta)$ , in which case a large number of samples is required to  
 193 obtain a good sample approximation. This difficulty can be circumvented by adopting a multi-level  
 194 approach (Rubinstein and Kroese 2016). For the case of component reliability problems, i.e., when

195 the structure failure event  $F$  is comprised of a single first-passage failure event, we have developed  
 196 an efficient multi-level strategy to determine the IS density of  $\Theta$  by the CE method (Kanjilal et al.  
 197 2021). Here we extend this method to deal with series systems.

### 198 Multi-level CE method

The multi-level CE method solves the optimization problem in Eq. (12) by defining a sequence of target densities  $\{h_{\Theta}^{[k]}(\theta), k = 0, \dots, L\}$ , which starts from the nominal density  $p_{\Theta}(\theta)$  and gradually approaches the optimal IS density  $h_{\Theta}^*(\theta)$ . Consider the sequence of PDFs defined according to the expression

$$h_{\Theta}^{[k]}(\theta) = \frac{1}{C_k} P_{F|\Theta}(\theta)^{\gamma_k} p_{\Theta}(\theta), \quad (13)$$

199 where  $0 = \gamma_0 < \gamma_1 < \dots < \gamma_L = 1$  and  $C_k = \int_{\theta \in \mathbb{R}^{n_{\theta}}} P_{F|\Theta}(\theta)^{\gamma_k} p_{\Theta}(\theta) d\theta$ . Note that  $h_{\Theta}^{[0]}(\theta) =$   
 200  $p_{\Theta}(\theta)$  and  $h_{\Theta}^{[L]}(\theta) = h_{\Theta}^*(\theta)$ . The parameters  $\{\gamma_k, k = 1, \dots, L\}$  ensure a smooth transition  
 201 between  $p_{\Theta}(\theta)$  and  $h_{\Theta}^*(\theta)$ . In the multi-level approach, the CE optimization is solved sequentially  
 202 for each of the intermediate target densities, which leads to a sequence of parameter vectors  
 203  $\{\nu^{[k]}, k = 1, \dots, L\}$ . The final parameter vector  $\nu^{[L]}$  should approximate well the solution of Eq.  
 204 (12).

205 The parameter vector  $\nu^{[k]}$  in each level is estimated by solving a CE optimization problem  
 206 that minimizes the KL divergence between  $h_{\Theta}^{[k]}(\theta)$  and  $h_{\Theta}(\theta; \nu)$ . The objective function of the  
 207 resulting optimization, i.e., the expectation  $E_{p_{\Theta}} [P_{F|\Theta}(\theta)^{\gamma_k} \ln(h_{\Theta}(\theta; \nu))]$ , is approximated with  
 208 IS using a set of samples  $\{\theta^{(i)}, i = 1, \dots, N\}$  distributed according to  $h_{\Theta}(\theta; \hat{\nu}^{[k-1]})$ , where  $\hat{\nu}^{[k-1]}$   
 209 is the estimate of  $\nu^{[k-1]}$  determined in the previous level. The stochastic optimization problem to  
 210 be solved in each intermediate level is therefore given by

$$211 \hat{\nu}^{[k]} = \operatorname{argmax}_{\mathbf{q} \in \mathcal{V}} \frac{1}{N} \sum_{i=1}^N \tilde{W}_k(\theta^{(i)}, \hat{\nu}^{[k-1]}) \ln(h_{\Theta}(\theta^{(i)}; \mathbf{q})), \quad (14)$$

212 with  $\tilde{W}_k(\theta, \hat{\nu}^{[k-1]}) = P_{F|\Theta}(\theta)^{\gamma_k} \frac{p_{\Theta}(\theta)}{h_{\Theta}(\theta; \hat{\nu}^{[k-1]})}$ . A default choice for  $h_{\Theta}(\theta; \hat{\nu}^{[0]})$  is the nominal density

213  $p_{\Theta}(\theta)$ . The smoothing parameter  $\gamma_k$  is selected adaptively such that the sample CoV  $\hat{\delta}_{\tilde{W}_k}$  of the  
 214 weights  $\left\{ \tilde{W}_k \left( \theta^{(i)}, \hat{\nu}^{[k-1]} \right), i = 1, \dots, N \right\}$  is equal to a target value  $\delta_{target}$ :

$$215 \quad \gamma_k = \underset{\gamma \in (\gamma_{k-1}, 1)}{\operatorname{argmin}} \left( \hat{\delta}_{\tilde{W}_k}(\gamma) - \delta_{target} \right)^2. \quad (15)$$

216 The choice of the value of  $\delta_{target}$  is discussed in (Papaioannou et al. 2016; Papaioannou et al. 2018).  
 217 In the present study we set  $\delta_{target}$  to 1.5. It is noted that Eq. (15) is equivalent to requiring that  
 218 the number of effective samples available to fit the parametric density at each sampling iteration is  
 219 equal to a target value for a given  $N$  (Latz et al. 2018). The effective sample size (ESS) is expressed  
 220 in terms of the CoV of the weights as  $ESS = N / \left( 1 + \hat{\delta}_{\tilde{W}_k}^2(\gamma) \right)$ . The adaptive procedure is stopped  
 221 when the value of  $\gamma_k$  determined based on Eq. (15) is equal to 1. After convergence at the  $L$ -th  
 222 step, the final parameter vector  $\hat{\nu}^{[L]}$  is determined by solving Eq. (14) with  $\gamma_L = 1$ . The sampling  
 223 density  $h_{\Theta}(\theta; \hat{\nu}^{[L]})$  is taken as the IS density of  $\Theta$  for estimating the probability of failure.

### 224 Estimation of the conditional probability of failure during CE optimization

225 Determination of the IS density  $h_{\Theta}(\theta; \hat{\nu}^{[L]})$  requires evaluation of the conditional failure  
 226 probability  $P_{F|\Theta}(\theta)$  for all samples of  $\Theta$  generated during CE optimization. In principle, one could  
 227 estimate  $P_{F|\Theta}(\theta)$  by MCS, e.g., by using the IS method in (Au and Beck 2001b). However, to ensure  
 228 smooth convergence of the CE method, the CoV of the IS estimator of  $P_{F|\Theta}(\theta)$  should be small.  
 229 This requires a sufficient number of samples to be used in the estimator, which, in turn, increases  
 230 the number of evaluations of the dynamical system. To alleviate the increase in computational  
 231 effort, we employ an analytical approximation of  $P_{F|\Theta}(\theta)$  during CE optimization.

232 Recall that in series system reliability problems, failure occurs when any one of the responses  $Z_i$   
 233 out-crosses its prescribed threshold  $z_i^*$  within the duration  $T$  of the random excitation. The analytical  
 234 approximation we adopt is based on the Poisson hypothesis for the number of out-crossing (Rice  
 235 1944; Melchers and Beck 2018). For the discrete-time setting described earlier, this approximation  
 236 is given by

$$237 \quad P_{F|\Theta}(\theta) = 1 - \exp \left( - \sum_{k=2}^{nT} \alpha(t_k; \mathbf{z}^*, \theta) \Delta t \right), \quad (16)$$

238 where  $\mathbf{z}^* = \{z_1^*, \dots, z_m^*\}$  is the vector of response thresholds and  $\alpha(t_k; \mathbf{z}^*, \boldsymbol{\theta})$  is the out-crossing  
 239 rate of the vector process  $\mathbf{Z}(t, \boldsymbol{\theta}, \boldsymbol{\Xi}) = \{Z_1(t, \boldsymbol{\theta}, \boldsymbol{\Xi}), \dots, Z_m(t, \boldsymbol{\theta}, \boldsymbol{\Xi})\}$  across the  $m$ -dimensional  
 240 double-sided barrier  $\{|Z_i| = z_i^*, i = 1, \dots, m\}$  at time  $t = t_k$ . This rate is written as the sum of the  
 241 individual out-crossing rates of the scalar processes over their respective barrier (Li and Melchers  
 242 1993; Song and Der Kiureghian 2006)

$$243 \quad \alpha(t_k; \mathbf{z}^*, \boldsymbol{\theta}) = \sum_{i=1}^m \alpha_i(t_k; \mathbf{z}^*, \boldsymbol{\theta}), \quad (17)$$

244 where  $\alpha_i(t_k; \mathbf{z}^*, \boldsymbol{\theta})$  denotes the out-crossing rate of the process  $Z_i(t, \boldsymbol{\theta}, \boldsymbol{\Xi})$  across the surface  $S_i =$   
 245  $\{\mathbf{Z} : |Z_i| = z_i^*, |Z_j| < z_j^* \forall j \neq i\}$  (representing  $i$ -th mode of failure) at time  $t = t_k$ . For double-  
 246 sided barrier,  $\alpha_i(t_k; \mathbf{z}^*, \boldsymbol{\theta})$  is further expressed as  $\alpha_i(t_k; \mathbf{z}^*, \boldsymbol{\theta}) = \alpha_i^+(t_k; \mathbf{z}^*, \boldsymbol{\theta}) + \alpha_i^-(t_k; \mathbf{z}^*, \boldsymbol{\theta})$ , where  
 247  $\alpha_i^+(t_k; \mathbf{z}^*, \boldsymbol{\theta})$  and  $\alpha_i^-(t_k; \mathbf{z}^*, \boldsymbol{\theta})$  denote the rates of up- and down- crossings of the process  $Z_i(t, \boldsymbol{\theta}, \boldsymbol{\Xi})$   
 248 across the thresholds  $z_i^*$  and  $-z_i^*$ , respectively. For a linear system subjected to a zero mean Gaussian  
 249 process excitation, the response  $Z_i(t, \boldsymbol{\theta}, \boldsymbol{\Xi})$  is a Gaussian random process (this follows directly from  
 250 Eq. (2)). Furthermore, due to the zero initial condition, the response process has a zero mean. In  
 251 this situation,  $\alpha_i^+(t_k; \mathbf{z}^*, \boldsymbol{\theta}) = \alpha_i^-(t_k; \mathbf{z}^*, \boldsymbol{\theta})$  holds, which leads to

$$252 \quad \alpha_i(t_k; \mathbf{z}^*, \boldsymbol{\theta}) = 2\alpha_i^+(t_k; \mathbf{z}^*, \boldsymbol{\theta}). \quad (18)$$

253 The up-crossing rate  $\alpha_i^+(t_k; \mathbf{z}^*, \boldsymbol{\theta})$  is calculated based on the generalized Rice formula (Belyaev  
 254 1968)

$$255 \quad \alpha_i^+(t_k; \mathbf{z}^*, \boldsymbol{\theta}) = \int_{S_i^*} \int_0^\infty \dot{z}_i f_{\dot{Z}_i Z_i \tilde{\mathbf{Z}}}(\dot{z}_i, z_i^*, \tilde{\mathbf{z}}; t_k) d\dot{z}_i d\tilde{\mathbf{z}}, \quad (19)$$

256 where  $\tilde{\mathbf{Z}}$  is the  $(m-1)$ -dimensional random process obtained from the vector process  $\mathbf{Z}$  by removing  
 257 its  $i$ -th component, i.e.,  $\tilde{\mathbf{Z}} = \{Z_1, \dots, Z_{i-1}, Z_{i+1}, \dots, Z_m\}$ ,  $S_i^* = \{\tilde{\mathbf{Z}} : |Z_j| < z_j^*\}$  is the  $(m-1)$ -  
 258 dimensional subspace defined on the hyperplane of the  $i$ -th face  $Z_i = z_i^*$ ,  $\dot{Z}_i$  is the time derivative  
 259 process of  $Z_i$  and  $f_{\dot{Z}_i Z_i \tilde{\mathbf{Z}}}(\cdot; t_k)$  is the joint PDF of  $\dot{Z}_i$ ,  $Z_i$  and  $\tilde{\mathbf{Z}}$  at the same time instant. An  
 260 analytical approach for evaluating the above integral is derived in (Song and Der Kiureghian 2006).

261 The approach requires repeated conditioning of the PDF  $f_{Z_i \bar{Z}}(\cdot; t_k)$  and is practically feasible  
 262 when  $m$ , i.e., the number of components of the series system, is small. Application of this approach  
 263 within the framework of the CE method has been explored in (Kanjilal et al. 2020). An alternative  
 264 approach, applicable to systems with large number of components, is to solve  $\alpha_i^+(t_k; \mathbf{z}^*, \boldsymbol{\theta})$  by  
 265 obtaining an upper bound for the integral. This bound reduces the multi-dimensional integral in  
 266 Eq. (19) into a one-dimensional integral over the real line and is given by (Li and Melchers 1993)

$$267 \quad \alpha_i^+(t_k; \mathbf{z}^*, \boldsymbol{\theta}) \leq f_{Z_i}(z_i^*; t_k) \int_{-\infty}^{\infty} \left[ \sigma_i \phi\left(-\frac{y}{\sigma_i}\right) + y \Phi\left(\frac{y}{\sigma_i}\right) \right] \frac{1}{\beta_i} \phi\left(\frac{y - \mu_i}{\beta_i}\right) dy, \quad (20)$$

268 where  $\Phi(\cdot)$  and  $\phi(\cdot)$  are the cumulative distribution function and the PDF of a standard normal  
 269 random variable, respectively.  $f_{Z_i}(z_i^*; t_k)$  denotes the marginal pdf of  $Z_i$  at  $t = t_k$  evaluated at  
 270  $Z_i = z_i^*$ ,

$$271 \quad f_{Z_i}(z_i^*; t_k) = \frac{1}{\sigma_{Z_i}} \phi\left(\frac{z_i^* - \mu_{Z_i}}{\sigma_{Z_i}}\right), \quad (21)$$

272  $\sigma_i$  denotes the standard deviation of  $\dot{Z}_i | \{Z_i = z_i^*, \bar{\mathbf{Z}} = \bar{\mathbf{z}}\}$  at  $t = t_k$ ,

$$273 \quad \sigma_i = \sqrt{\text{Var}[\dot{Z}_i | Z_i = z_i^*, \bar{\mathbf{Z}} = \bar{\mathbf{z}}]} = \sigma_{\dot{Z}_i} \sqrt{1 - \rho_i^2}, \quad (22)$$

274 and the parameters  $\mu_i$  and  $\beta_i$  are given by:

$$275 \quad \begin{aligned} \mu_i &= \mu_{Z_i} + \rho_{Z_i \dot{Z}_i} \frac{\sigma_{\dot{Z}_i}}{\sigma_{Z_i}} (z_i^* - \mu_{Z_i}) \\ \beta_i &= \sigma_{\dot{Z}_i} \sqrt{\rho_i^2 - \rho_{Z_i \dot{Z}_i}^2}. \end{aligned} \quad (23)$$

276 In Eqs. (21)-(23),  $\mu_{Z_i}$  and  $\mu_{\dot{Z}_i}$  denote the mean of  $Z_i$  and  $\dot{Z}_i$ ,  $\sigma_{Z_i}$  and  $\sigma_{\dot{Z}_i}$  denote the standard devia-  
 277 tion of  $Z_i$  and  $\dot{Z}_i$ ,  $\rho_{Z_i \dot{Z}_i}$  denotes the correlation coefficient of  $Z_i$  and  $\dot{Z}_i$  and  $\rho_i = \sqrt{\Sigma_{\dot{Z}_i \mathbf{Z}}^T \Sigma_{\mathbf{Z} \mathbf{Z}}^{-1} \Sigma_{\dot{Z}_i \mathbf{Z}}} / \sigma_{\dot{Z}_i}$ .  
 278 Here  $\Sigma_{\mathbf{Z} \mathbf{Z}}$  is the covariance matrix of the vector process  $\mathbf{Z}$  and  $\Sigma_{\dot{Z}_i \mathbf{Z}}$  is the covariance of  $\dot{Z}_i$  and  $\mathbf{Z}$ .  
 279 The above statistics are computed at  $t = t_k$  by direct analysis of Eq. (3).

280 In this work, we derive an analytical solution of the integral in Eq. (20) that facilitates faster

281 computation of the upper bound of  $\alpha_i^+(t_k; \mathbf{z}^*, \boldsymbol{\theta})$ . The details of this derivation are provided in  
 282 Appendix I. By substituting the solution into Eq. (20) and applying Eqs. (17) and (18) we get the  
 283 following upper bound of the out-crossing rate of the series system

$$284 \quad \alpha(t_k; \mathbf{z}^*, \boldsymbol{\theta}) \leq 2 \sum_{i=1}^m f_{Z_i}(z_i^*; t_k) \left\{ \sqrt{\sigma_i^2 + \beta_i^2} \phi \left( \frac{\mu_i}{\sqrt{\sigma_i^2 + \beta_i^2}} \right) + \mu_i \Phi \left( \frac{\mu_i}{\sqrt{\sigma_i^2 + \beta_i^2}} \right) \right\}. \quad (24)$$

285 Substitution of Eq. (24) into Eq. (16) leads to an upper bound on the conditional failure probability  
 286  $P_{F|\Theta}(\boldsymbol{\theta})$ . We evaluate  $P_{F|\Theta}(\boldsymbol{\theta})$  approximately using this upper bound during CE optimization. The  
 287 resulting procedure for determining the IS density of  $\Theta$  is described in Algorithm 1. The analytical  
 288 approximation reduces the computational cost at the expense of accuracy. However, numerical  
 289 studies show that the IS density obtained based on this approach gives fairly accurate estimates of  
 290 the unconditional failure probability. The IS estimator of  $P_{F|\Theta}(\boldsymbol{\theta})$  is applied only during reliability  
 291 estimation (as described in the next section), after the final IS density of  $\Theta$  is obtained.

292 Finally, we remark that the Poisson approximation for the number of out-crossings used in Eq.  
 293 (16) may not work well for all linear systems. When the threshold levels are small and/or the response  
 294 processes have a narrow bandwidth, the assumption of independent out-crossings underlying the  
 295 Poisson approximation is not justified and could result in erroneous estimates. In such cases, the  
 296 IS density of the uncertain parameters constructed by the CE method will be sub-optimal, which  
 297 will increase the sampling CoV of the IS estimator of the series system failure probability. This  
 298 issue can be addressed by applying Vanmarcke's formula for evaluating the out-crossing rate in  
 299 Eq. (16). Vanmarcke's formula, proposed in (Vanmarcke 1975) and further developed in (Di Paola  
 300 1985; Michaelov et al. 1999; Barbato and Conte 2011), provides an improved estimate of the  
 301 failure probability by taking into account the dependence between the out-crossing events of the  
 302 scalar responses  $\{Z_i(t, \boldsymbol{\theta}, \boldsymbol{\Xi}), i = 1, \dots, m\}$  across their respective threshold levels. This leads to a  
 303 modified out-crossing rate for the vector process  $\mathbf{Z}(t, \boldsymbol{\theta}, \boldsymbol{\Xi})$ , deduced by multiplying  $\alpha_i(t; \mathbf{z}^*, \boldsymbol{\theta})$  in  
 304 Eq. (17) with a correction term that is equal to the ratio of the out-crossing rates of the response  
 305  $Z_i(t, \boldsymbol{\theta}, \boldsymbol{\Xi})$  and its envelope process across the threshold  $z_i^*$ . The upper bound on the out-crossing

306 rate  $\alpha(t; \mathbf{z}^*, \boldsymbol{\theta})$  of the system responses in Eq. (24) needs to be modified accordingly. A detailed  
 307 description of the correction term is provided in (Song and Der Kiureghian 2006).

---

**Algorithm 1:** Determination of IS density of  $\Theta$  by the multi-level CE method

---

1 **input:**  
 2 | Sample size  $N$ .  
 3 | Choice of parametric density  $h_{\Theta}(\boldsymbol{\theta}; \boldsymbol{\nu})$ .  
 4 | Target CoV of the weights at each intermediate level,  $\delta_{target}$ .  
 5 **initialization:**  
 6 | Set  $k = 0$ .  
 7 | Select  $h_{\Theta}(\boldsymbol{\theta}; \hat{\boldsymbol{\nu}}^{[0]})$  as the nominal density  $p_{\Theta}(\boldsymbol{\theta})$ .  
 8 **repeat:**  
 9 | Set  $k = k + 1$ .  
 10 | Generate independent samples  $\{\boldsymbol{\theta}^{(i)}, i = 1, \dots, N\}$  from  $h_{\Theta}(\boldsymbol{\theta}; \hat{\boldsymbol{\nu}}^{[k-1]})$ .  
 11 | Evaluate the out-crossing rates  $\{\alpha(t_k; \mathbf{z}^*, \boldsymbol{\theta}^{(i)}), i = 1, \dots, N\}$  for the random samples at  
 the discrete time instants  $\{t_k, k = 1, \dots, n_T\}$  based on the upper bound in Eq. (24).  
 12 | Substitute the upper bounds of the out-crossing rates computed in the previous step  
 into Eq. (16) to compute an approximate estimate (an upper bound) of the conditional  
 failure probabilities  $\{P_{F|\Theta}(\boldsymbol{\theta}^{(i)}), i = 1, \dots, N\}$ .  
 13 | Compute the likelihood ratio  $\left\{ \frac{p_{\Theta}(\boldsymbol{\theta}^{(i)})}{h_{\Theta}(\boldsymbol{\theta}^{(i)}; \hat{\boldsymbol{\nu}}^{[k-1]})}, i = 1, \dots, N \right\}$  for the random samples.  
 14 | Solve the optimization problem in Eq. (15) to determine  $\gamma_k$ .  
 Note that the conditional first-passage probabilities and the likelihood ratios  
 computed in the previous steps are used to evaluate the sample CoV of the weights  
 $\left\{ \tilde{W}_k(\boldsymbol{\theta}^{(i)}, \hat{\boldsymbol{\nu}}^{[k-1]}), i = 1, \dots, N \right\}$ . Further simulations are not needed in this step.  
 15 | Determine  $\hat{\boldsymbol{\nu}}^{[k]}$  by solving the optimization problem in Eq. (14).  
 16 **while**  $\gamma_k < 1$   
 17 **output:**  
 18 |  $L = k$  and  $h_{\Theta}(\boldsymbol{\theta}; \hat{\boldsymbol{\nu}}^{[L]}) = \text{IS density of } \Theta$ .

---

308 **Choice of parametric distribution family**

309 The failure domain in series system reliability problems is comprised of multiple important  
 310 regions, each representing the domain of the component failure events. Due to this, the optimal IS  
 311 density  $h_{\Theta}^*(\boldsymbol{\theta})$  is typically multi-modal. Therefore, to adequately represent  $h_{\Theta}^*(\boldsymbol{\theta})$ , the parametric  
 312 density  $h_{\Theta}(\boldsymbol{\theta}; \boldsymbol{\nu})$  should also have a multi-modal behavior. We consider two types of mixture  
 313 distributions as the parametric family: the Gaussian mixture distribution and the von Mises-Fisher-  
 314 Nakagami mixture distribution. Recall that  $\Theta = \{\Theta_1; \dots; \Theta_{n_{\theta}}\}$  is the vector of basic random

315 variables that model the uncertain structural parameters. In reliability analysis, it is common  
 316 practice to consider that the components of  $\Theta$  are independent and standard normally distributed.  
 317 If the structural parameters are mutually dependent and/or follow a non-Gaussian distribution, they  
 318 can be generated by an iso-probabilistic transformation of independent standard normal random  
 319 variables (Hohenbichler and Rackwitz 1981; Der Kiureghian and Liu 1986). Therefore, without  
 320 loss of generality, we assume that  $\Theta$  is an  $n_\theta$ -dimensional standard Gaussian random vector, i.e.,  
 321  $p_\Theta(\boldsymbol{\theta}) = \prod_{j=1}^{n_\theta} p_{\Theta_j}(\theta_j)$ , where for every  $j$ ,  $p_{\Theta_j}(\theta_j)$  is a one-dimensional standard Gaussian PDF  
 322 for  $\Theta_j$ .

### 323 *Gaussian mixture distribution*

324 The PDF of a Gaussian mixture (GM) model is defined as the sum of a number of Gaussian  
 325 PDFs, each of them multiplied by a weighing factor:

$$326 \quad f_{\text{GM}}(\boldsymbol{\theta}; \boldsymbol{\nu}) = \sum_{s=1}^{n_M} \pi_s f_{\text{G}}(\boldsymbol{\theta}; \boldsymbol{\mu}_s, \boldsymbol{\Sigma}_s), \quad (25)$$

327 where  $f_{\text{G}}(\boldsymbol{\theta}; \boldsymbol{\mu}_s, \boldsymbol{\Sigma}_s)$  is the  $s$ -th Gaussian PDF with mean  $\boldsymbol{\mu}_s$  and covariance matrix  $\boldsymbol{\Sigma}_s$  and  $\{\pi_s; s =$   
 328  $1, \dots, n_M\}$  are normalized weights satisfying the condition  $\sum_{s=1}^{n_M} \pi_s = 1$ . The parameter vector in  
 329 this case is given by  $\boldsymbol{\nu} = \{\pi_s, \boldsymbol{\mu}_s, \boldsymbol{\Sigma}_s; s = 1, \dots, n_M\}$ , where  $\pi_s$  is scalar-valued,  $\boldsymbol{\mu}_s$  is a vector of  
 330 dimension  $n_\theta$  and  $\boldsymbol{\Sigma}_s$  is an  $n_\theta \times n_\theta$  symmetric matrix. This results in a total of  $n_M \frac{n_\theta(n_\theta+3)}{2} + (n_M - 1)$   
 331 unknown parameters in the parametric density. The parameter vector is determined in every level  
 332 of the CE method by solving the optimization problem in Eq.(14). The optimal solution in each  
 333 level is obtained by substituting  $h_\Theta(\boldsymbol{\theta}; \boldsymbol{\nu}) = f_{\text{GM}}(\boldsymbol{\theta}; \boldsymbol{\nu})$  in Eq. (14), and equating the gradient of the  
 334 objective function with respect to the unknown parameters to zero.

335 For the special case of  $n_M = 1$ , an exact analytical solution of the optimization problem can  
 336 be obtained (Rubinstein and Kroese 2016). For the general case of  $n_M > 1$ , the optimization  
 337 is solved iteratively using an appropriate numerical scheme. The recent study in (Geyer et al.  
 338 2019) employs the fact that the CE optimization problem can be viewed as a weighted maximum  
 339 likelihood estimation problem to derive a modified expectation-maximization (EM) algorithm. In

340 the present study, we adopt this approach to solve Eq. (14). The EM procedure and the updating  
 341 rules of  $\hat{\nu}^{[k]}$  for the GM model are described in (Geyer et al. 2019) and are not further discussed  
 342 here.

343 *von Mises-Fisher-Nakagami mixture distribution*

344 The CE method with Gaussian densities performs poorly in high-dimensional problems, i.e.,  
 345 in problems where the number  $n_\theta$  of uncertain structural parameters is large. This is due to two  
 346 reasons: the first is the degeneracy of the importance weight function  $W(\theta)$  in high-dimensions  
 347 (Au and Beck 2003; Katafygiotis and Zuev 2008). The second reason is the number of parameters  
 348 in the GM model, which increases quadratically with  $n_\theta$ . This results in a rapid increase in the  
 349 number of samples per level  $N$  required to obtain an adequate estimate of the optimal parameter  
 350 values.

351 Papaioannou et al. (Papaioannou et al. 2019) introduce the von-Mises-Fisher-Nakagami  
 352 (vMFN) density as an alternative choice of the parametric family in the CE method. This paramet-  
 353 ric density is more efficient in high-dimensions. For series system reliability analysis, one should  
 354 use a von-Mises-Fisher-Nakagami mixture (vMFNM), whose PDF is defined in terms of the polar  
 355 coordinates of the standard normal random vector  $\Theta$ :

$$356 \quad f_{\text{vMFNM}}([r \mathbf{a}]; \boldsymbol{\nu}) = \sum_{s=1}^{n_M} \pi_s f_{\text{vMFN}}([r \mathbf{a}]; \boldsymbol{\mu}_s, \kappa_s, \psi_s, \Omega_s), \quad (26)$$

357 where the sample pair  $\{r \mathbf{a}\}$  represents the polar coordinates (radius and direction) of  $\theta$  and  
 358  $f_{\text{vMFN}}([r \mathbf{a}], \boldsymbol{\mu}_s, \kappa_s, \psi_s, \Omega_s)$  is the  $s$ -th vMFN density with parameters  $\{\boldsymbol{\mu}_s, \kappa_s, \psi_s, \Omega_s\}$  and normal-  
 359 ized weight  $\pi_s$ . The vMFN PDF in Eq. (26) is (Papaioannou et al. 2019)

$$360 \quad f_{\text{vMFN}}([r \mathbf{a}]; \boldsymbol{\mu}_s, \kappa_s, \psi_s, \Omega_s) = f_{\text{N}}(r; \psi_s, \Omega_s) f_{\text{vMF}}(\mathbf{a}; \boldsymbol{\mu}_s, \kappa_s), \quad (27)$$

361 where  $f_{\text{vMF}}(\mathbf{a}; \boldsymbol{\mu}_s, \kappa_s)$  is the PDF of a von Mises-Fisher distribution with mean direction  $\boldsymbol{\mu}_s$  ( $\|\boldsymbol{\mu}_s\| =$   
 362 1) and concentration parameter  $\kappa_s \geq 0$  and  $f_{\text{N}}(r; \psi_s, \Omega_s)$  is the PDF of a Nakagami distribution

363 with shape parameter  $\psi_s \geq 0.5$  and spread parameter  $\Omega_s > 0$ . The analytical expressions of  
 364  $f_{\text{vMF}}(\mathbf{a}; \boldsymbol{\mu}_s, \kappa_s)$  and  $f_{\text{N}}(r; \psi_s, \Omega_s)$  can be found in (Wang and Song 2016; Papaioannou et al. 2019).

365 When the vMFN distribution is used within the CE method, the unknown parameter vector  
 366 to be estimated by CE optimization is given by  $\boldsymbol{\nu} = \{[\boldsymbol{\mu}_s, \kappa_s, \psi_s, \Omega_s]; s = 1, \dots, n_M\}$ . Here all  
 367 parameters are scalar-valued, with the exception of  $\{\boldsymbol{\mu}_s; s = 1, \dots, n_M\}$ , which are vectors of  
 368 dimension  $n_\theta$ . Thus, the total number of parameters to be estimated in each sampling iteration is  
 369  $n_M(n_\theta + 3) + (n_M - 1)$ , which increases only linearly with  $n_\theta$ . The optimal parameter vector in  
 370 each level of the CE method is determined by substituting  $h_{\Theta}(\boldsymbol{\theta}; \boldsymbol{\nu}) = f_{\text{vMFNM}}([\mathbf{r} \ \mathbf{a}]; \boldsymbol{\nu})$  in Eq. (14)  
 371 and equating the derivative of the objective function with respect to the unknown parameters to  
 372 zero. We apply the EM algorithm to solve the CE optimization problem. The EM procedure and  
 373 the updating rules of  $\hat{\boldsymbol{\nu}}^{[k]}$  for the vMFNM are described in (Papaioannou et al. 2019) and are not  
 374 further discussed here.

## 375 ESTIMATION OF PROBABILITY OF FAILURE BY IMPORTANCE SAMPLING

376 The IS density of the uncertain structural parameters derived in the previous section is applied  
 377 to estimate the probability of failure of the series system. To this end, we write the unconditional  
 378 failure probability of Eq. (6) in the modified form

$$379 \quad P_F = \int_{\boldsymbol{\theta} \in \mathbb{R}^{n_\theta}} P_{F|\Theta}(\boldsymbol{\theta}) \frac{P_{\Theta}(\boldsymbol{\theta})}{h_{\Theta}(\boldsymbol{\theta}; \hat{\boldsymbol{\nu}}^{[L]})} h_{\Theta}(\boldsymbol{\theta}; \hat{\boldsymbol{\nu}}^{[L]}) d\boldsymbol{\theta}, \quad (28)$$

380 where  $h_{\Theta}(\boldsymbol{\theta}; \hat{\boldsymbol{\nu}}^{[L]})$  denotes the IS density of the uncertain parameters  $\Theta$  obtained using the CE  
 381 method and  $P_{F|\Theta}(\boldsymbol{\theta})$  is the system probability of failure conditional on  $\Theta = \boldsymbol{\theta}$ . The conditional  
 382 failure probability is defined in Eq. (7). To ensure reliable and efficient estimation of  $P_F$  based on  
 383 Eq. (28), we evaluate  $P_{F|\Theta}(\boldsymbol{\theta})$  by IS sampling.

384 Consider the discrete time representation of the dynamical system introduced earlier. Let the  
 385 failure event  $F_{i,k}$  denote out-crossing of the threshold level  $z_i^*$  by the  $i$ -th absolute structural response,  
 386  $Z_i$ , at time instant  $t = t_k$ . From the definition of the system failure event in Eqs. (4) and (5), it follows  
 387 that occurrence of any one of the elementary failure events  $\{F_{i,k}; i = 1, \dots, m, k = 1, \dots, n_T\}$  leads

388 to failure of the structure. Hence, the failure event of the series system is an union of the elementary  
 389 failure events, i.e.,  $F = \bigcup_{i=1}^m \bigcup_{k=1}^{n_T} F_{i,k}$ . In order to evaluate  $P_{F|\Theta}(\theta)$  by IS, we introduce an IS  
 390 density of the random vector  $\Xi$  characterizing the input excitation, and modify the integral in Eq.  
 391 (7) to

$$392 \quad P_{F|\Theta}(\theta) = \int_{\xi \in \mathbb{R}^{n_\xi}} \mathbf{I}\{(\theta, \xi) \in F\} \frac{p_\Xi(\xi)}{h_\Xi(\xi|\theta)} h_\Xi(\xi|\theta) d\xi, \quad (29)$$

393 where  $h_\Xi(\xi|\theta)$  denotes the IS density of  $\Xi$  conditional on  $\Theta = \theta$ . Since the structure is deterministic  
 394 for a given value of the uncertain parameters, the sampling density  $h_\Xi(\xi|\theta)$  can be designed  
 395 based on available IS methods for dynamic reliability estimation of deterministic structures. For  
 396 the particular case of deterministic linear structures subjected to Gaussian process excitation, an  
 397 efficient IS density of  $\Xi$  is suggested in (Au and Beck 2001b). We employ this IS density to evaluate  
 398  $P_{F|\Theta}(\theta)$ . Accordingly, we define  $h_\Xi(\xi|\theta)$  as a weighted sum of Gaussian PDFs truncated over the  
 399 domain of the elementary failure events:

$$400 \quad h_\Xi(\xi|\theta) = \sum_{i=1}^m \sum_{k=1}^{n_T} w_{i,k}(\theta) p_\Xi(\xi|\{(\theta, \xi) \in F_{i,k}\}) = \sum_{i=1}^m \sum_{k=1}^{n_T} w_{i,k}(\theta) \frac{p_\Xi(\xi) \mathbf{I}\{(\theta, \xi) \in F_{i,k}\}}{\Pr[F_{i,k}|\Theta = \theta]}, \quad (30)$$

401 where  $w_{i,k}(\theta)$  are normalized weights given by

$$402 \quad w_{i,k}(\theta) = \frac{\Pr[F_{i,k}|\Theta = \theta]}{\sum_{r=1}^m \sum_{s=1}^{n_T} \Pr[F_{r,s}|\Theta = \theta]}. \quad (31)$$

403 The probability of occurrence of  $F_{i,k}$  conditional on  $\Theta = \theta$  is calculated according to the expression  
 404  $\Pr[F_{i,k}|\Theta = \theta] = 2\Phi(-h_i^*/\|\mathbf{r}_{i,k}(\theta)\|)$ , where  $\mathbf{r}_{i,k}(\theta)$  is as defined in Eq. (3).

405 Substituting  $P_{F|\Theta}(\theta)$  in Eq. (28) with the integral in Eq. (29), we obtain the following  
 406 expression for  $P_F$ :

$$407 \quad P_F = \int_{\theta \in \mathbb{R}^{n_\theta}} \int_{\xi \in \mathbb{R}^{n_\xi}} \left\{ \frac{\tilde{P}(\theta)}{\sum_{i=1}^m \sum_{k=1}^{n_T} \mathbf{I}\{(\theta, \xi) \in F_{i,k}\}} W(\theta) \right\} h_{\Theta, \Xi}(\theta, \xi) d\xi d\theta, \quad (32)$$

408 where  $h_{\Theta, \Xi}(\theta, \xi) = h_\Xi(\xi|\theta) h_\Theta(\theta; \hat{\nu}^{[L]})$  is the joint IS density of  $\Theta$  and  $\Xi$ ,  $W(\theta) = \frac{p_\Theta(\theta)}{h_\Theta(\theta; \hat{\nu}^{[L]})}$  is the

409 importance weight function associated with  $\Theta$  and  $\tilde{P}(\theta) = \sum_{i=1}^m \sum_{k=1}^{n_T} \Pr [F_{i,k} | \Theta = \theta]$  is the sum  
 410 of probabilities of the elementary failure events  $\{F_{i,k}; i = 1, \dots, m, k = 1, \dots, n_T\}$  conditional on  
 411  $\Theta = \theta$ . The probability of failure of the series system is therefore estimated by IS as

$$412 \quad \hat{P}_F = \frac{1}{N_R} \sum_{j=1}^{N_R} \frac{\tilde{P}(\theta^{(j)})}{\sum_{i=1}^m \sum_{k=1}^{n_T} \mathbb{I}\{(\theta^{(j)}, \xi^{(j)}) \in F_{i,k}\}} W(\theta^{(j)}), \quad (33)$$

413 where  $\{(\theta^{(j)}, \xi^{(j)}), j = 1, \dots, N_R\}$  are independent samples of the structural parameters and ex-  
 414 citation distributed according to  $h_{\Theta, \Xi}(\theta, \xi) = h_{\Xi}(\xi | \theta) h_{\Theta}(\theta; \hat{\nu}^{[L]})$ . In order to generate a sample  
 415  $(\theta^{(j)}, \xi^{(j)})$  from  $h_{\Theta, \Xi}(\theta, \xi)$ , we first generate  $\theta^{(j)}$  from the IS density  $h_{\Theta}(\theta; \hat{\nu}^{[L]})$ . The corre-  
 416 sponding sample  $\xi^{(j)}$  is then generated from the conditional IS density  $h_{\Xi}(\xi | \theta^{(j)})$  according to the  
 417 algorithm described in (Au and Beck 2001b; Kanjilal et al. 2021).

## 418 NUMERICAL INVESTIGATIONS

419 We investigate the performance of the CE-based IS (CE-IS) method by means of two numerical  
 420 examples. The first considers a two-story linear shear frame, with two uncertain structural parame-  
 421 ters, subjected to a stationary Gaussian white noise. The system failure event is defined in terms of  
 422 three components. This constitutes a simplified problem in terms of both the number of uncertain  
 423 structural parameters and component failure modes, and is intended to illustrate different aspects of  
 424 the proposed method. The second example considers a six-story three-bay moment-resisting frame  
 425 driven by a filtered non-stationary Gaussian process excitation. This problem demonstrates the  
 426 performance of the method in a more complicated setting where the system consists of 22 uncertain  
 427 structural parameters and 24 components. In both examples,  $\Theta$  is a vector of independent standard  
 428 normal random variables. The uncertain structural parameters are generated from  $\Theta$  by means of  
 429 iso-probabilistic transformations.

430 The performance of the CE-IS method is assessed in terms of the sample mean and sample  
 431 CoV of the estimates of  $P_F$ , denoted by  $\hat{P}_F$  and  $\delta_{\hat{P}_F}$  in this section, and in terms of the number of  
 432 dynamical system evaluations required by the method.  $N_{CE}$  denotes the total number of samples  
 433 of  $\Theta$  needed to determine the IS density of the uncertain parameters using the CE method.  $N_R$

434 denotes the number of samples of  $(\Theta, \Xi)$  used to obtain a sample estimate of  $P_F$  during reliability  
435 estimation, i.e., for evaluating Eq. (33). The dynamical system is required to be evaluated for every  
436 sample realization of  $\Theta$  to determine the impulse response functions. During CE optimization, the  
437 impulse response functions of the critical responses  $Z_i$  and their velocities  $\dot{Z}_i$  are post-processed  
438 to evaluate the analytical approximation of  $P_{F|\Theta}(\theta)$ . In the reliability estimation step, the impulse  
439 response functions of  $Z_i$  are convoluted with a sample realization of the input excitation to obtain  
440 a realization of the response time-histories. In the considered examples, the input excitation is  
441 represented by a scalar Gaussian process, i.e.,  $l = 1$ . Hence, for every generated sample of  
442 the uncertain parameters, the impulse response functions of  $Z_i$  and  $\dot{Z}_i$  are obtained from a single  
443 dynamic analysis. Therefore,  $N_{CE}$  and  $N_R$  also indicate the number of dynamical system evaluations  
444 needed in the CE optimization step and the reliability estimation step, respectively.  $N_T = N_{CE} + N_R$   
445 is the total number of system evaluations required to obtain an estimate of  $P_F$ . The performance  
446 measures are averaged over 50 independent simulation runs. The reference values of the probability  
447 of failure are obtained by large-scale direct MCS.

448 While implementing the CE-IS method, the sample size  $N_R$  in the reliability estimation step is  
449 selected using two approaches. In the first approach,  $N_R$  is taken equal to the number of samples  
450 per level for CE optimization, i.e.,  $N_R = N$ . In the second approach,  $N_R$  is adapted on the fly to  
451 ensure that an estimate of the CoV of the IS estimate of  $P_F$  is smaller than a specified target value  
452  $\delta_{\hat{P}_F}^*$ . The adaptive variant of the IS estimator is implemented according to the procedure described  
453 in (Kanjilal et al. 2021).

#### 454 **A two-story linear shear frame**

455 The first example involves a two-story linear shear frame which is excited by a stochastic ground  
456 acceleration. The structure, idealized as a mass-spring-dashpot system with 2 degrees of freedom, is  
457 depicted in Fig. 1. The system has been previously studied in (Valdebenito et al. 2014). Each floor  
458 possesses a mass of  $m = 30\text{Mg}$ . The stiffness parameters  $\{k_i; i = 1, 2\}$  are modeled as independent  
459 uniform random variables with marginal distribution  $k_i \sim \text{U}[12, 28]\text{MN/m}$ . A classical damping of  
460 4% is assumed for the two modes. The ground acceleration  $f(t)$  is modeled as a stationary Gaussian

461 white noise of duration  $T = 15\text{s}$  and spectral intensity  $S = 10^{-4}\text{m}^2/\text{s}^3$ . The stochastic excitation is  
462 discretized at time intervals of  $\Delta t = 0.01\text{s}$ , i.e.,  $n_T = 1501$ . The random vector  $\Xi$  characterizing  
463  $f(t)$  consists of the sequence of i.i.d. standard normal random variables  $\{\Xi_k, k = 1, \dots, n_T\}$  that  
464 generate the white noise at the discrete time instants, i.e.,  $\{f(t_k) = \sqrt{2\pi S/\Delta t}\Xi_k, k = 1, \dots, n_T\}$ .  
465 Three response measures are considered:  $Z_1$  = absolute displacement of the first floor, and  $Z_2$  =  
466 inter-story drift between first and second floors and  $Z_3$  = absolute displacement of the top floor.  
467 The objective is to estimate the probability that any one of these responses exceeds a corresponding  
468 threshold  $z_i^*$  over the duration of the random excitation.

469 We consider two choices of the response thresholds: (i) case 1:  $(z_1^*, z_2^*, z_3^*) = (0.006, 0.006, 0.006)\text{m}$ ,  
470 this is the case studied in (Valdebenito et al. 2014) and (ii) case 2:  $(z_1^*, z_2^*, z_3^*) = (0.004, 0.003, 0.006)\text{m}$ .  
471 The reference value of the probability of failure in both cases is estimated by direct MCS with  $10^7$   
472 samples. The performance of the CE-IS method is investigated for the following parametric fam-  
473 ilies: single Gaussian (S-G) distribution, single vMFN (S-vMFN) distribution, Gaussian mixture  
474 (GM) distribution and vMFN mixture (vMFNM) distribution. For the mixture models,  $n_M = 3$   
475 densities are considered to account for the three component failure modes of the series system. In  
476 the present example, where the number of uncertain structural parameters is  $n_\theta = 2$ , the parameter  
477 vector  $\nu$  for S-G and S-vMFN distributions consists of 5 unknown parameters, whereas for GM  
478 and vMFNM distributions it consists of 17 unknown parameters.

479 Fig. 2 shows samples from the IS densities of  $\Theta$  for case 1 obtained using the different parametric  
480 densities. The IS densities are fitted using  $N = 250$  samples per level during CE optimization. It is  
481 seen that the optimal IS density in this case is uni-modal. This can be attributed to the fact that the  
482 contribution to the system failure probability comes primarily from one of the three components,  
483 i.e., there is one dominant component failure mode (the top floor displacement) for the considered  
484 values of the response thresholds. As a consequence, a uni-model parametric density is able to  
485 adequately represent the important region of the failure domain in the  $\Theta$ -space. The use of mixture  
486 distributions does not offer any additional advantage in this case. This is further substantiated by  
487 Table 1, where we report the results of reliability analysis and the computational effort for  $N =$

488 250 and 1000 samples per level. All four parametric densities require two steps on average to  
 489 converge to the failure domain, as is indicated by the value of  $N_{CE}$ . The computational effort  
 490 required to determine the IS density of  $\Theta$  is comparable among the different parametric families.  
 491 The probability of failure estimates in Table 1 are obtained using a fixed number of samples (equal  
 492 to  $N$ ) in the IS estimator, i.e.,  $N_R$  = number of samples per level during CE optimization. The  
 493 reference value of the probability of system failure is  $1.79 \times 10^{-3}$  with a CoV of 0.8%. For all  
 494 four parametric densities, the sample mean of the probability estimates obtained by the CE-IS  
 495 method compare well with the reference solution. In terms of the sample CoV of the estimates, the  
 496 performance of the method is similar for all choices of the parametric density.

497 The IS densities of  $\Theta$  in case 2, i.e., for  $(z_1^*, z_2^*, z_3^*) = (0.004, 0.003, 0.006)m$ , are illustrated  
 498 in Fig. 3. The failure domain has multiple important regions, as is indicated by the multi-modal  
 499 nature of the optimal IS density  $h_{\Theta}^*(\theta)$ . For the GM and vMFNM distributions, it can be seen  
 500 that the three mixture components can describe the failure domain sufficiently accurate and that  
 501 majority of the samples are located near the modes of the optimal IS density, which are the regions  
 502 that have a higher contribution to the probability of failure. In contrast, the samples from the  
 503 S-G and S-vMFN distributions are more dispersed with a higher fraction of these located in the  
 504 less important regions, i.e., regions which have less contribution to the failure probability. As a  
 505 consequence, the uni-modal parametric densities are less efficient than the mixture distributions  
 506 for this case. This is further substantiated by the simulation results in Table 2. The results are  
 507 obtained with  $N = 250$  samples per level. The values of  $N_{CE}$  indicate that for all choices of the  
 508 parametric density, the CE method requires two steps on average to converge. We evaluate the  
 509 IS estimator for  $P_F$  with both non-adaptive and adaptive selection of  $N_R$ . The two choices of  $N_R$   
 510 are indicated by  $N_R$ -NonAdap and  $N_R$ -Adap in Table 2. The results for  $N_R$ -Adap correspond to a  
 511 target CoV of  $\delta_{\hat{P}_F}^* = 0.05$ . The reference value of the probability of system failure is  $4.70 \times 10^{-3}$   
 512 with a CoV of 0.5%. The sample mean of the probability estimates obtained with the two choices  
 513 of  $N_R$  are similar for all parametric densities. Although we observe a small bias in comparison  
 514 with the reference solution, the estimates given by the CE-IS method are sufficiently accurate for

515 practical use. In terms of the sample CoV of the estimates and the computational effort, the mixture  
516 distributions perform better. For  $N_R$ -NonAdap, it is seen that the CoV of the estimates obtained  
517 using the GM and vMFNM distributions are smaller than the ones obtained using the S-G and  
518 S-vMFN distributions. For  $N_R$ -Adap, the GM and vMFNM distributions require lesser number of  
519 dynamic system evaluations to converge to the target CoV of 5%. The superior performance of  
520 the mixture distributions is due to the greater accuracy in describing the multi-modal nature of the  
521 failure domain.

522 We investigate the effect of the sample size per level  $N$  on the performance of the method. For  
523 this, different values of  $N$  in the range 125-1000 are considered. The study is conducted for case  
524 2 using the mixture distributions as the parametric family. The sample means of the probability  
525 estimates are similar to those given in Table 2 and hence are not reported separately. The sample  
526 CoV of the estimates and the computational effort is depicted in Fig. 4. It is observed that the  
527 number of levels required for the CE optimization to converge remains the same (on average equal  
528 to two) for all values of  $N$ . Hence, the computational effort needed for optimization,  $N_{CE}$ , increases  
529 monotonically with  $N$ . The difference between the vertical coordinates of the dotted line and the  
530 solid lines corresponds to  $N_R$ , the average number of dynamical system evaluations used in the  
531 reliability estimation step. With increase in  $N$ , the number of effective samples of  $\Theta$  available to  
532 fit the parametric densities at each intermediate level increases. This leads to better estimation of  
533 the parameters in the IS density of  $\Theta$ . For  $N_R$ -NonAdap, where  $N_R = N$ , an increase in  $N$  also  
534 implies an increase in the number of samples of  $(\Theta, \Xi)$  used to obtain a sample estimate of  $P_F$   
535 during reliability estimation. Due to these factors, the sample CoV of the probability estimates for  
536  $N_R$ -NonAdap decreases as  $N$  increases. For  $N_R$ -Adap, it is seen that the sample size for reliability  
537 estimation initially decreases as  $N$  increases. This is due to the sub-optimality in the IS density of  $\Theta$   
538 obtained with a small  $N$ , which leads to a greater computational effort during reliability estimation  
539 necessary to meet the prescribed  $\delta_{\hat{P}_F}^*$ . As  $N$  increases, one obtains improved estimates of the  
540 parameter vector, and the number of samples for reliability estimation starts decreasing. Beyond  
541 a certain value of  $N$ ,  $N = 500$  in this example,  $N_R$  is nearly constant, which indicates that the IS

542 density of  $\Theta$  obtained using 500 samples per level is sufficiently optimal, and a further increase  
 543 in  $N$  does not give any additional advantage during reliability estimation. The sample CoV of the  
 544 probability estimates for  $N_R$ -Adap remains close to the prescribed  $\delta_{\hat{P}_F}^*$  for all  $N$ . Finally, Fig. 4  
 545 shows that the IS estimator with adaptive selection of  $N_R$  requires a smaller number of dynamical  
 546 system evaluations to meet a prescribed CoV. It is seen that the GM with  $N_R$ -Adap requires only  
 547 1350 system evaluations to achieve a sample CoV less than 5%, whereas with  $N_R$ -NonAdap similar  
 548 accuracy is obtained with approximately 3000 system evaluations. A similar observation is made  
 549 for the vMFNM distribution. This indicates that if the goal is to achieve a desired value of the  
 550 sample CoV, the adaptive variant of the IS estimator is more efficient provided that the number of  
 551 samples per level  $N$  is chosen appropriately. Similar results as in Fig. 4 are observed for component  
 552 reliability analysis of randomly excited uncertain linear structures where the failure event is defined  
 553 by the first-passage of a single critical response across a prescribed threshold (Kanjilal et al. 2021).

#### 554 **A moment-resisting steel frame**

555 We consider the six-story three-bay moment-resisting steel frame shown in Fig. 5. The structure  
 556 has been previously analysed in an example given in (Au and Beck 2001b), where deterministic  
 557 structural parameters are considered. The frame is represented by a two-dimensional linear finite  
 558 element model. The members connecting the joints of the frame are described by two-noded beam  
 559 elements with two translational DOF and one rotational DOF per node. The equation of motion  
 560 of the structure is obtained after applying static condensation wherein only the DOFs representing  
 561 the horizontal displacement of the columns are retained. The frame members have different cross-  
 562 sections, which are denoted by  $\{C_i; i = 1, \dots, 6\}$  (for columns) and  $\{G_i; i = 1, \dots, 3\}$  (for girders)  
 563 in Fig. 5. For each floor, the same section is used for all the girders. The member sections are  
 564 taken from Example 2 in (Au and Beck 2001b). The Young's modulus of the members vary with  
 565 cross-section:  $\{E_i; i = 1, \dots, 3\}$  denote the modulus of the girder sections  $\{G_i; i = 1, \dots, 3\}$  and  
 566  $\{E_i; i = 4, \dots, 9\}$  denote the modulus of column sections  $\{C_i; i = 1, \dots, 6\}$ .  $\{E_i; i = 1, \dots, 9\}$   
 567 are modeled by independent log-normal random variables with mean 200 GPa and CoV 10%. A  
 568 lumped mass model is applied, wherein the mass of the frame members and the contribution from

569 the dead loads are lumped at the nodes of the frame. These point masses are considered as uncertain  
570 and are modeled by log-normal random variables with mean values given in Table 3 and CoV 10%.  
571 Rayleigh damping is assumed so that the first two modes have the same critical damping ratio,  
572 which is modeled by a log-normal random variable with mean 0.04 and CoV 10%. Hence, the  
573 number of uncertain structural parameters is  $n_{\theta} = 22$ .

574 The structure is excited by a stochastic ground acceleration  $f(t)$  applied in the horizontal  
575 direction. We adopt the characterization of the random excitation given in (Au and Beck 2001b)  
576 and model  $f(t)$  by a modulated Clough-Penzin filtered white noise:

$$577 \quad f(t) = \omega_d^2 x_d(t) + 2\eta_d \omega_d \dot{x}_d(t) - \omega_g^2 x_g(t) - 2\eta_g \omega_g \dot{x}_g(t), \quad (34)$$

578 where  $\{x_d(t) \ \dot{x}_d(t) \ x_g(t) \ \dot{x}_g(t)\}^T$  are the states of the filter defined by the linear system:

$$579 \quad \begin{aligned} \ddot{x}_d(t) + 2\eta_d \omega_d \dot{x}_d(t) + \omega_d^2 x_d(t) &= e(t)N(t) \\ \ddot{x}_g(t) + 2\eta_g \omega_g \dot{x}_g(t) + \omega_g^2 x_g(t) &= 2\eta_d \omega_d \dot{x}_d(t) + \omega_d^2 x_d(t) \\ x_d(0) = 0, \dot{x}_d(0) = 0, x_g(0) = 0, \dot{x}_g(0) &= 0. \end{aligned} \quad (35)$$

580 In the above equation,  $N(t)$  is a Gaussian white noise with zero mean and spectral intensity  
581  $S = 1 \times 10^{-3} \text{m}^2/\text{s}^3$ . The numerical values of the filter parameters are taken to be  $\omega_d = 15.7 \text{ rad/s}$ ,  
582  $\eta_d = 0.6$ ,  $\omega_g = 17.5 \text{ rad/s}$  and  $\eta_g = 0.8$ . The envelope function is given by  $e(t)$ :

$$583 \quad e(t) = \begin{cases} 0 & \text{for } t \leq 0\text{s} \\ (t/4)^2 & \text{for } 0\text{s} \leq t \leq 4\text{s} \\ 1 & \text{for } 4\text{s} \leq t \leq 14\text{s} \\ \exp(-(t-14)^2/2) & \text{for } t \geq 14\text{s} \end{cases} \quad (36)$$

584 A duration of  $T = 30\text{s}$  and a sampling time interval of  $\Delta t = 0.02\text{s}$  are used in computing the  
585 response of the structure. Therefore, the total number of standard Gaussian random variables in

586 the discrete approximation of  $f(t)$  is  $n_T = 1501$ .

### 587 *Peak inter-story drift ratio*

588 Here we consider the probability that the peak inter-story drift ratio at any column exceeds a  
589 specified threshold level  $z^*$  in (%). The responses  $\{Z_i; i = 1, \dots, m\}$  thus consist of the inter-story  
590 drift ratios of all columns connecting the floors, resulting in  $m = 24$  critical responses. As the  
591 number of uncertain structural parameters is high, the vMFN density is selected as the parametric  
592 family in the CE-IS method. Since all columns in a floor experience nearly the same inter-story  
593 drift, a significant overlap of the respective failure domains is expected. To adequately describe the  
594 failure domains of all columns in the six stories, a mixture distribution with  $n_M = 6$  components is  
595 considered. The parameter vector  $\nu$  thus consists of 155 unknown parameters.

596 The simulation results for threshold levels  $z^* = 0.5, 0.75$  and 1% are given in Table 4. The IS  
597 density of  $\Theta$  is determined using  $N = 500$  samples per level during CE optimization. The values of  
598  $N_{CE}$  reported in the table indicate that the number of levels required for the optimization to converge  
599 increases with the threshold level. The probability of failure is estimated using both choices of  $N_R$ .  
600 The results for  $N_R$ -Adap correspond to a target CoV of  $\delta_{\hat{P}_F}^* = 0.10$ . Failure probability estimates  
601 for both  $N_R$ -NonAdap and  $N_R$ -Adap are comparable and agree well with the reference solution. The  
602 sample CoV of the probability estimates for  $N_R$ -Adap remain close to the target value  $\delta_{\hat{P}_F}^* = 0.10$ .  
603 For  $N_R$ -NonAdap, the probability estimates for higher threshold levels have smaller CoV than for  
604 lower thresholds, whereas for  $N_R$ -Adap the number of dynamical system evaluations required to  
605 achieve the target CoV decreases with increase in the threshold level. For  $z^* = 0.5\%$  the method  
606 performs poorly; crude MCS would result in a similar CoV with a lower computational effort of  
607 approximately 625 samples. The poor performance of the CE-IS method for  $z^* = 0.5\%$  can be due  
608 to two reasons. First, the out-crossing rate-based analytical approximation is used to evaluate the  
609 conditional probability  $P_{F|\Theta}(\theta)$  during CE optimization. It is known that the Poisson assumption of  
610 the number of out-crossing can perform poorly for low threshold levels. This leads to a sub-optimal  
611 IS density of the uncertain structural parameters for  $z^* = 0.5\%$ . The second reason could be that  
612 the applied distribution model might not be able to approximate well the optimal IS density. The

613 latter issue can be addressed by increasing the number of terms in the mixture distribution.

#### 614 *Peak floor acceleration*

615 Here we consider the failure probability that the peak floor acceleration over all stories exceeds  
616 a specified threshold level  $z^*$  (in g). Since the horizontal displacement of the girders is obtained  
617 by linear interpolation of the nodal displacements of the beam elements, this probability is equal  
618 to the failure probability that the absolute horizontal acceleration at any one of the nodes of the  
619 frame exceeds the threshold level  $z^*$ . There are thus  $m = 24$  critical responses  $\{Z_i; i = 1, \dots, m\}$   
620 corresponding to the horizontal acceleration at the 24 nodes of the structure. The probability of  
621 failure is estimated for threshold levels  $z^* = 0.2, 0.3$  and  $0.4g$ . The simulation results obtained  
622 using a vMFNM distribution with  $n_M = 6$  mixture components is given in Table 5. A sample size  
623 of  $N = 500$  is used per level during CE optimization. Similar to the case of peak inter-story drifts,  
624 the results show that the computational effort required to determine the IS density of the uncertain  
625 structural parameters increases with the threshold level. For  $z^* = 0.2$  and  $0.3g$ , the probability  
626 of failure estimates obtained from the CE-IS method agree well with the reference solution. For  
627  $z^* = 0.4g$ , a small under-estimation is observed; however, for this threshold the sampling uncertainty  
628 of the reference solution is significant. It is seen that the sample CoV of the probability estimates  
629 for  $N_R$ -NonAdap with  $N_R = 500$  is comparable to that for  $N_R$ -Adap with  $\delta_{\hat{P}_F}^* = 0.10$ . However,  
630 the number of dynamical system evaluations required to obtain the estimates with  $N_R$ -Adap is less.  
631 This indicates that for  $N = 500$  samples per level the IS estimator with adaptive selection of  $N_R$  is  
632 more efficient.

#### 633 **CONCLUDING REMARKS**

634 This contribution presents an adaptive IS method to estimate the series system reliability of  
635 uncertain linear structures subject to Gaussian loading. The main contribution is the introduction  
636 of an efficient IS density of the uncertain structural parameters. We determine this IS density by  
637 the CE method through minimizing the KL divergence between the theoretically optimal IS density  
638 and a chosen parametric family of probability distributions. Based on an upper bound on the joint  
639 out-crossing rate of the output responses, a closed-form analytical approximation of the system

640 failure probability conditional on a fixed value of the structural parameters is derived. The use  
641 of the analytical approximation enables smooth convergence of the CE optimization problem. A  
642 joint IS density of the uncertain structural parameters and the random excitation is considered to  
643 estimate the probability of failure. The numerical results indicate that the proposed approach is  
644 efficient and accurate.

645 We investigate the performance of alternative parametric distribution models, depending on  
646 the number of uncertain structural parameters and failure modes. In series systems, where the  
647 structural failure event is a union of multiple first-passage failures, the optimal IS density of the  
648 uncertain parameters is usually multi-modal in nature. In such cases, a mixture distribution offers  
649 more flexibility in approximating the optimal IS density. This is demonstrated in our numerical  
650 studies, where we compare the performance of uni-modal and mixture distribution models from  
651 the Gaussian and the vMFN density family. The mixture distributions outperform the uni-modal  
652 distributions both in terms of the coefficient of variation of the failure probability estimate and the  
653 computational effort. In terms of dimensionality of the problems, i.e., the number of uncertain  
654 structural parameters  $n_\theta$  involved, we note that the proposed method remains applicable in high  
655 dimensions. However, fitting the IS density of the uncertain parameters by CE minimization  
656 becomes computationally expensive due to increase in the number of unknown parameters in the  
657 parametric densities. This increase is quadratic in  $n_\theta$  for the GM distribution and linear in  $n_\theta$  for  
658 the vMFNM distribution. Hence, to adequately fit the parametric IS density in high dimensions, a  
659 larger number of samples will be required in each level of the CE method. The required sample  
660 size scales approximately the same as the number of unknown parameters. In small dimensions,  
661 the GM and vMFNM distributions exhibit similar efficiency. In high dimensions, the vMFNM  
662 distribution is more efficient.

663 As future research, it is interesting to further develop the method for application to non-  
664 linear dynamical systems. In the presence of non-linearity, the structural response processes are  
665 non-Gaussian. An extension of the method to non-Gaussian response processes poses two key  
666 challenges. The first lies in obtaining an analytical approximation of the failure probability condi-

667 tional on the structural parameters, which is required to determine the IS density of the uncertain  
668 parameters by CE minimization. In this regard, application of the Poisson approximation requires  
669 knowledge of out-crossing rates of non-Gaussian response processes, which is not straight-forward  
670 to obtain. An estimate of the conditional failure probability for non-linear systems can be obtained,  
671 for example, by stochastic averaging (dos Santos et al. 2019) or tail-equivalent linearization (Fu-  
672 jimura and Der Kiureghian 2007) techniques. However, these methods are computationally too  
673 costly for repeated evaluations in the context of the proposed CE-IS method and would need to be  
674 adapted. The second challenge lies in constructing an effective IS density of the random excitation  
675 to evaluate the conditional failure probability during reliability estimation. Some approaches can  
676 be found in (Schuëller et al. 2004a; Kanjilal and Manohar 2019), but also here additional research  
677 is necessary to enable their implementation into the proposed approach.

#### 678 **Data Availability Statement**

679 All data, models, or code that support the findings of this study are available from the corre-  
680 sponding author upon reasonable request.

#### 681 **Acknowledgments**

682 This work is supported by the Alexander von Humboldt Foundation.

#### 683 **Appendix I. Evaluation of the upper bound of $\alpha_i^+(t_k; \mathbf{z}^*, \boldsymbol{\theta})$**

684 The integral in the upper bound of the up-crossing rate  $\alpha_i^+(t_k; \mathbf{z}^*, \boldsymbol{\theta})$  in Eq. (20) is given by

$$685 \quad J = \int_{-\infty}^{\infty} \left[ \sigma_i \phi \left( -\frac{y}{\sigma_i} \right) + y \Phi \left( \frac{y}{\sigma_i} \right) \right] \frac{1}{\beta_i} \phi \left( \frac{y - \mu_i}{\beta_i} \right) dy, \quad (37)$$

686 where  $\sigma_i$ ,  $\mu_i$  and  $\beta_i$  are as defined in Eqs. (22) and (23). In order to derive an analytical solution  
687 of  $J$ , we consider the change of variables  $u = (y - \mu_i)/\beta_i$ . Then Eq. (37) can be re-expressed as

$$\begin{aligned}
J &= \int_{-\infty}^{\infty} \left[ \sigma_i \phi \left( -\frac{\beta_i u + \mu_i}{\sigma_i} \right) + (\beta_i u + \mu_i) \Phi \left( \frac{\beta_i u + \mu_i}{\sigma_i} \right) \right] \phi(u) du \\
&= \sigma_i \int_{-\infty}^{\infty} \phi \left( -\frac{\beta_i u + \mu_i}{\sigma_i} \right) \phi(u) du + \beta_i \int_{-\infty}^{\infty} \Phi \left( \frac{\beta_i u + \mu_i}{\sigma_i} \right) u \phi(u) du \\
&\quad + \mu_i \int_{-\infty}^{\infty} \Phi \left( \frac{\beta_i u + \mu_i}{\sigma_i} \right) \phi(u) du \\
&= \sigma_i J_1 + \beta_i J_2 + \mu_i J_3
\end{aligned} \tag{38}$$

There exist well-known expressions for evaluating integrals of functions of normal densities (Owen 1980). Using these results we get the following analytical expressions for  $J_1$ ,  $J_2$  and  $J_3$ :

$$\begin{aligned}
J_1 &= \int_{-\infty}^{\infty} \phi \left( -\frac{\beta_i u + \mu_i}{\sigma_i} \right) \phi(u) du = \frac{\sigma_i}{\sqrt{\beta_i^2 + \sigma_i^2}} \phi \left( \frac{\mu_i}{\sqrt{\beta_i^2 + \sigma_i^2}} \right) \\
J_2 &= \int_{-\infty}^{\infty} \Phi \left( \frac{\beta_i u + \mu_i}{\sigma_i} \right) u \phi(u) du = \frac{\beta_i}{\sqrt{\beta_i^2 + \sigma_i^2}} \phi \left( \frac{\mu_i}{\sqrt{\beta_i^2 + \sigma_i^2}} \right) \\
J_3 &= \int_{-\infty}^{\infty} \Phi \left( \frac{\beta_i u + \mu_i}{\sigma_i} \right) \phi(u) du = \Phi \left( \frac{\mu_i}{\sqrt{\beta_i^2 + \sigma_i^2}} \right)
\end{aligned} \tag{39}$$

Substitution of Eq. (39) into Eq. (38) leads to the result

$$J = \sqrt{\beta_i^2 + \sigma_i^2} \phi \left( \frac{\mu_i}{\sqrt{\beta_i^2 + \sigma_i^2}} \right) + \mu_i \Phi \left( \frac{\mu_i}{\sqrt{\beta_i^2 + \sigma_i^2}} \right) \tag{40}$$

## REFERENCES

- Au, S. K. and Beck, J. L. (2001a). "Estimation of small failure probabilities in high dimensions by subset simulation." *Probabilistic Engineering Mechanics*, 16(4), 263–277.
- Au, S. K. and Beck, J. L. (2001b). "First excursion probabilities for linear systems by very efficient importance sampling." *Probabilistic Engineering Mechanics*, 16(3), 193–207.
- Au, S. K. and Beck, J. L. (2003). "Importance sampling in high dimensions." *Structural Safety*, 25(2), 139–163.

701 Barbato, M. and Conte, J. P. (2011). “Structural reliability applications of nonstationary spectral  
702 characteristics.” *Journal of engineering mechanics*, 137(5), 371–382.

703 Belyaev, Y. K. (1968). “On the number of exits across the boundary of a region by a vector stochastic  
704 process.” *SIAM Journal of Theory of Probability & Its Applications*, 13(2), 320–324.

705 Byun, J.-E. and Song, J. (2020). “Bounds on reliability of larger systems by linear programming  
706 with delayed column generation.” *Journal of Engineering Mechanics*, 146(4), 04020008.

707 Der Kiureghian, A. and Liu, P. L. (1986). “Structural reliability under incomplete probability  
708 information.” *ASCE Journal of Engineering Mechanics*, 112(1), 85–104.

709 Di Paola, M. (1985). “Transient spectral moments of linear systems.” *SM archives*, 10(3), 225–243.

710 dos Santos, K. R., Kougioumtzoglou, I. A., and Spanos, P. D. (2019). “Hilbert transform–based  
711 stochastic averaging technique for determining the survival probability of nonlinear oscillators.”  
712 *Journal of Engineering Mechanics*, 145(10), 04019079.

713 Fujimura, K. and Der Kiureghian, A. (2007). “Tail-equivalent linearization method for nonlinear  
714 random vibration.” *Probabilistic Engineering Mechanics*, 22(1), 63–76.

715 Geyer, S., Papaioannou, I., and Straub, D. (2019). “Cross entropy-based importance sampling using  
716 Gaussian densities revisited.” *Structural Safety*, 76, 15–27.

717 Hohenbichler, M. and Rackwitz, R. (1981). “Non-normal dependent vectors in structural safety.”  
718 *ASCE Journal of the Engineering Mechanics Division*, 107(6), 1227–1238.

719 Jensen, H. A. and Valdebenito, M. A. (2007). “Reliability analysis of linear dynamical systems  
720 using approximate representations of performance functions.” *Structural Safety*, 29(3), 222–237.

721 Kanjilal, O. and Manohar, C. S. (2019). “Estimation of time-variant system reliability of nonlinear  
722 randomly excited systems based on the Girsanov transformation with state-dependent controls.”  
723 *Nonlinear Dynamics*, 95(2), 1693–1711.

724 Kanjilal, O., Papaioannou, I., and Straub, D. (2020). “Series system reliability estimation of  
725 randomly excited uncertain linear structures by cross entropy-based importance sampling.” *Proc.*  
726 *7th Asian-Pacific Symposium on Structural Reliability and Its Applications*, Vol. 8, 136–41.

727 Kanjilal, O., Papaioannou, I., and Straub, D. (2021). “Cross entropy-based importance sampling

728 for first-passage probability estimation of randomly excited linear structures with parameter  
729 uncertainty.” *Structural Safety*, 91, 102090.

730 Katafygiotis, L. and Cheung, S. H. (2004). “Wedge simulation method for calculating the reliability  
731 of linear dynamical systems.” *Probabilistic Engineering Mechanics*, 19(3), 229–238.

732 Katafygiotis, L. and Cheung, S. H. (2006). “Domain decomposition method for calculating the  
733 failure probability of linear dynamic systems subjected to Gaussian stochastic loads.” *Journal of*  
734 *Engineering Mechanics*, 132(5), 475–486.

735 Katafygiotis, L. S. and Zuev, K. M. (2008). “Geometric insight into the challenges of solving high-  
736 dimensional reliability problems.” *Probabilistic Engineering Mechanics*, 23(2-3), 208–218.

737 Koutsourelakis, P. S., Pradlwarter, H. J., and Schuëller, G. I. (2004). “Reliability of structures in  
738 high dimensions, part I: algorithms and applications.” *Probabilistic Engineering Mechanics*,  
739 19(4), 409–417.

740 Latz, J., Papaioannou, I., and Ullmann, E. (2018). “Multilevel sequential Monte Carlo for Bayesian  
741 inverse problems.” *Journal of Computational Physics*, 368, 154–178.

742 Li, C. Q. and Melchers, R. E. (1993). “Outcrossings from convex polyhedrons for nonstationary  
743 Gaussian processes.” *ASCE Journal of Engineering Mechanics*, 119(11), 2354–2361.

744 Melchers, R. E. and Beck, A. T. (2018). *Structural reliability analysis and prediction*. John Wiley  
745 & Sons.

746 Michaelov, G., Sarkani, S., and Lutes, L. (1999). “Spectral characteristics of nonstationary random  
747 processes—a critical review.” *Structural safety*, 21(3), 223–244.

748 Misraji, M. A., Valdebenito, M. A., Jensen, H. A., and Mayorga, C. F. (2020). “Application of  
749 directional importance sampling for estimation of first excursion probabilities of linear structural  
750 systems subject to stochastic Gaussian loading.” *Mechanical Systems and Signal Processing*,  
751 139, 106621.

752 Owen, D. B. (1980). “A table of normal integrals.” *Communications in Statistics-Simulation and*  
753 *Computation*, 9(4), 389–419.

754 Papaioannou, I., Breitung, K., and Straub, D. (2018). “Reliability sensitivity estimation with

755 sequential importance sampling.” *Structural Safety*, 75, 24–34.

756 Papaioannou, I., Geyer, S., and Straub, D. (2019). “Improved cross entropy-based importance  
757 sampling with a flexible mixture model.” *Reliability Engineering & System Safety*, 191, 106564.

758 Papaioannou, I., Papadimitriou, C., and Straub, D. (2016). “Sequential importance sampling for  
759 structural reliability analysis.” *Structural Safety*, 62, 66–75.

760 Pradlwarter, H. J. and Schuëller, G. I. (2010). “Uncertain linear structural systems in dynamics:  
761 Efficient stochastic reliability assessment.” *Computers & Structures*, 88(1-2), 74–86.

762 Rice, S. O. (1944). “Mathematical analysis of random noise.” *Bell System Technical Journal*, 23(3),  
763 282–332.

764 Rubinstein, R. Y. and Kroese, D. P. (2016). *Simulation and the Monte Carlo method*, Vol. 10. John  
765 Wiley & Sons.

766 Schuëller, G., Pradlwarter, H., and Koutsourelakis, P. (2004a). “A critical appraisal of reliability  
767 estimation procedures for high dimensions.” *Probabilistic engineering mechanics*, 19(4), 463–  
768 474.

769 Schuëller, G. I., Pradlwarter, H. J., and Koutsourelakis, P. S. (2004b). “A critical appraisal of  
770 reliability estimation procedures for high dimensions.” *Probabilistic Engineering Mechanics*,  
771 19(4), 463–474.

772 Song, J. and Der Kiureghian, A. (2003). “Bounds on system reliability by linear programming.”  
773 *Journal of Engineering Mechanics*, 129(6), 627–636.

774 Song, J. and Der Kiureghian, A. (2006). “Joint first-passage probability and reliability of systems  
775 under stochastic excitation.” *ASCE Journal of Engineering Mechanics*, 132(1), 65–77.

776 Valdebenito, M. A., Jensen, H. A., and Labarca, A. A. (2014). “Estimation of first excursion  
777 probabilities for uncertain stochastic linear systems subject to Gaussian load.” *Computers &*  
778 *Structures*, 138, 36–48.

779 Vanmarcke, E. H. (1975). “On the distribution of the first-passage time for normal stationary random  
780 processes.” *Journal of Applied Mechanics*, 42(1), 215–220.

781 Wang, Z. and Song, J. (2016). “Cross entropy-based adaptive importance sampling using von

Mises-Fisher mixture for high dimensional reliability analysis.” *Structural Safety*, 59, 42–52.

**List of Tables**

783

784 1 Failure probability estimates of two-story linear shear frame - case 1. Results  
 785 obtained by the CE-IS method using the S-G, GM, S-vMFN and vMFNM distri-  
 786 butions. The reference value of probability of failure estimated from  $10^7$  direct  
 787 Monte Carlo samples is  $1.79 \times 10^{-3}$  with a CoV of 0.8% . . . . . 36

788 2 Failure probability estimates of two-story linear shear frame - case 2. Results  
 789 obtained by the CE-IS method using the S-G, GM, S-vMFN and vMFNM distri-  
 790 butions with  $N = 250$  samples per level. The results for  $N_R$ -Adap correspond to a  
 791 target CoV of  $\delta_{\hat{P}_F}^* = 0.05$ . The reference value of probability of failure estimated  
 792 from  $10^7$  direct Monte Carlo samples is  $4.70 \times 10^{-3}$  with a CoV of 0.5% . . . . . 37

793 3 Probabilistic description of the point masses in moment-resisting steel frame. The  
 794 point masses follow log-normal distribution with mean values reported in the table  
 795 and CoV of 10%. . . . . 38

796 4 Failure probability estimates for peak inter-story drift ratio of moment-resisting  
 797 steel frame. Results from CE-IS method with  $N_R$ -Adap correspond to a target CoV  
 798 of  $\delta_{\hat{P}_F}^* = 0.10$ .  $N = 500$  samples used per level during CE optimization. Reference  
 799 solution estimated by  $2 \times 10^6$  direct Monte Carlo samples. . . . . 39

800 5 Failure probability estimates for peak floor acceleration of moment-resisting steel  
 801 frame. Results from CE-IS method with  $N_R$ -Adap correspond to a target CoV of  
 802  $\delta_{\hat{P}_F}^* = 0.10$ .  $N = 500$  samples used per level during CE optimization. Reference  
 803 solution estimated by  $2 \times 10^6$  direct Monte Carlo samples. . . . . 40

**TABLE 1.** Failure probability estimates of two-story linear shear frame - case 1. Results obtained by the CE-IS method using the S-G, GM, S-vMFN and vMFNM distributions. The reference value of probability of failure estimated from  $10^7$  direct Monte Carlo samples is  $1.79 \times 10^{-3}$  with a CoV of 0.8%

	$N = 250$					$N = 1000$				
	$\hat{P}_F$	$\delta_{\hat{P}_F}$	$N_{CE}$	$N_R$	$N_T$	$\hat{P}_F$	$\delta_{\hat{P}_F}$	$N_{CE}$	$N_R$	$N_T$
S-G	$1.69 \times 10^{-3}$	0.071	510	250	760	$1.71 \times 10^{-3}$	0.032	2000	1000	3000
GM	$1.71 \times 10^{-3}$	0.068	535	250	785	$1.71 \times 10^{-3}$	0.036	2020	1000	3020
S-vMFN	$1.69 \times 10^{-3}$	0.069	510	250	760	$1.70 \times 10^{-3}$	0.034	2040	1000	3040
vMFNM	$1.70 \times 10^{-3}$	0.068	520	250	770	$1.72 \times 10^{-3}$	0.032	2020	1000	3020

**TABLE 2.** Failure probability estimates of two-story linear shear frame - case 2. Results obtained by the CE-IS method using the S-G, GM, S-vMFN and vMFNM distributions with  $N = 250$  samples per level. The results for  $N_R$ -Adap correspond to a target CoV of  $\delta_{\hat{P}_F}^* = 0.05$ . The reference value of probability of failure estimated from  $10^7$  direct Monte Carlo samples is  $4.70 \times 10^{-3}$  with a CoV of 0.5%

	$N_{CE}$	$N_R$ -NonAdap				$N_R$ -Adap			
		$\hat{P}_F$	$\delta_{\hat{P}_F}$	$N_R$	$N_T$	$\hat{P}_F$	$\delta_{\hat{P}_F}$	$N_R$	$N_T$
S-G	515	$4.50 \times 10^{-3}$	0.174	250	765	$4.38 \times 10^{-3}$	0.050	1400	1915
GM	515	$4.40 \times 10^{-3}$	0.095	250	765	$4.41 \times 10^{-3}$	0.047	838	1353
S-vMFN	520	$4.25 \times 10^{-3}$	0.120	250	770	$4.43 \times 10^{-3}$	0.048	954	1474
vMFNM	530	$4.47 \times 10^{-3}$	0.106	250	780	$4.38 \times 10^{-3}$	0.045	842	1372

**TABLE 3.** Probabilistic description of the point masses in moment-resisting steel frame. The point masses follow log-normal distribution with mean values reported in the table and CoV of 10%.

Floor	Mean value of point mass ( $\times 10^3$ kg)	
	Exterior column	Interior column
2	60.4	81.0
3	53.3	78.1
4	51.9	76.0
5	51.7	75.8
6	50.1	73.5
Roof	44.6	63.1

**TABLE 4.** Failure probability estimates for peak inter-story drift ratio of moment-resisting steel frame. Results from CE-IS method with  $N_R$ -Adap correspond to a target CoV of  $\delta_{\hat{P}_F}^* = 0.10$ .  $N = 500$  samples used per level during CE optimization. Reference solution estimated by  $2 \times 10^6$  direct Monte Carlo samples.

$z^*$ (%)	CE-IS									direct MC	
	$N_R$ -NonAdap					$N_R$ -Adap				$P_F$	$\delta_{P_F}$
	$N_{CE}$	$\hat{P}_F$	$\delta_{\hat{P}_F}$	$N_R$	$N_T$	$\hat{P}_F$	$\delta_{\hat{P}_F}$	$N_R$	$N_T$		
0.5	500	$1.33 \times 10^{-1}$	0.173	500	1000	$1.28 \times 10^{-1}$	0.112	1203	1703	$1.31 \times 10^{-1}$	0.002
0.75	1000	$4.36 \times 10^{-3}$	0.137	500	1500	$4.21 \times 10^{-3}$	0.103	858	1858	$4.31 \times 10^{-3}$	0.011
1	1620	$7.61 \times 10^{-5}$	0.142	500	2120	$7.32 \times 10^{-5}$	0.090	696	2316	$7.70 \times 10^{-5}$	0.081

**TABLE 5.** Failure probability estimates for peak floor acceleration of moment-resisting steel frame. Results from CE-IS method with  $N_R$ -Adap correspond to a target CoV of  $\delta_{\hat{P}_F}^* = 0.10$ .  $N = 500$  samples used per level during CE optimization. Reference solution estimated by  $2 \times 10^6$  direct Monte Carlo samples.

$z^*$	CE-IS									direct MC	
	(g)	$N_R$ -NonAdap				$N_R$ -Adap				$P_F$	$\delta_{P_F}$
$N_{CE}$		$\hat{P}_F$	$\delta_{\hat{P}_F}$	$N_R$	$N_T$	$\hat{P}_F$	$\delta_{\hat{P}_F}$	$N_R$	$N_T$		
0.2	500	$1.09 \times 10^{-1}$	0.091	500	1000	$1.06 \times 10^{-1}$	0.093	392	892	$1.09 \times 10^{-1}$	0.002
0.3	1480	$2.21 \times 10^{-3}$	0.112	500	1980	$2.14 \times 10^{-3}$	0.080	302	1782	$2.21 \times 10^{-3}$	0.015
0.4	2120	$2.42 \times 10^{-5}$	0.098	500	2620	$2.40 \times 10^{-5}$	0.102	476	2596	$1.55 \times 10^{-5}$	0.180

804  
805  
806  
807  
808  
809  
810  
811  
812  
813  
814  
815  
816  
817  
818  
819  
820

## List of Figures

- 1 Two-story shear frame excited by stochastic ground acceleration  $f(t)$  . . . . . 42
- 2 Comparison of the IS density of the uncertain structural parameters in the standard normal space ( $\Theta$ -space) for two-story linear shear frame - case 1. The solid lines represent the contours of the optimal IS density  $h_{\Theta}^*(\theta)$ , which is estimated by direct MCS with  $10^7$  samples. The scattered points are samples of  $\Theta$  drawn from the IS density obtained by the CE-IS method. . . . . 43
- 3 Comparison of the IS density of the uncertain structural parameters in the standard normal space ( $\Theta$ -space) for two-story linear shear frame - case 2. The solid lines represent the contours of the optimal IS density  $h_{\Theta}^*(\theta)$ , which is estimated by direct MCS with  $10^7$  samples. The scattered points are samples of  $\Theta$  drawn from the IS density obtained by the CE-IS method. . . . . 44
- 4 Total computational effort  $N_T$  and the sample CoV  $\delta_{\hat{\rho}_F}$  as a function of  $N$  for two-story linear shear frame - case 2. The rows correspond to different parametric densities (a) GM distribution; (b) vMFNM distribution. Note that the dashed line does not reflect  $N_T$ , but the computational effort needed only for CE optimization. . . . . 45
- 5 Moment-resisting steel frame . . . . . 46

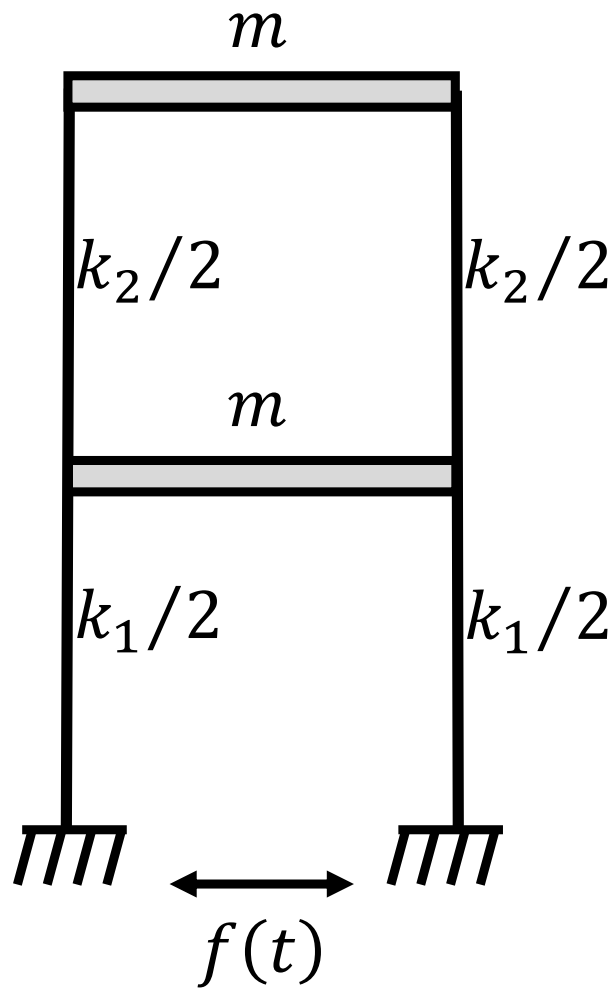


**Fig. 1.** Two-story shear frame excited by stochastic ground acceleration  $f(t)$

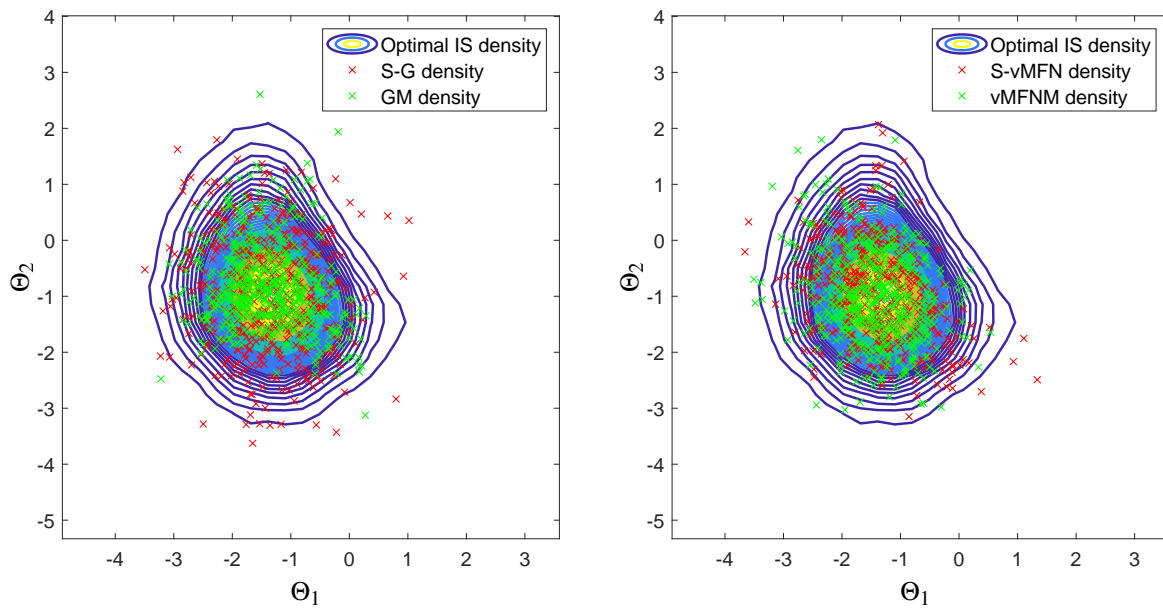


**Fig. 2.** Comparison of the IS density of the uncertain structural parameters in the standard normal space ( $\Theta$ -space) for two-story linear shear frame - case 1. The solid lines represent the contours of the optimal IS density  $h_{\Theta}^*(\theta)$ , which is estimated by direct MCS with  $10^7$  samples. The scattered points are samples of  $\Theta$  drawn from the IS density obtained by the CE-IS method.

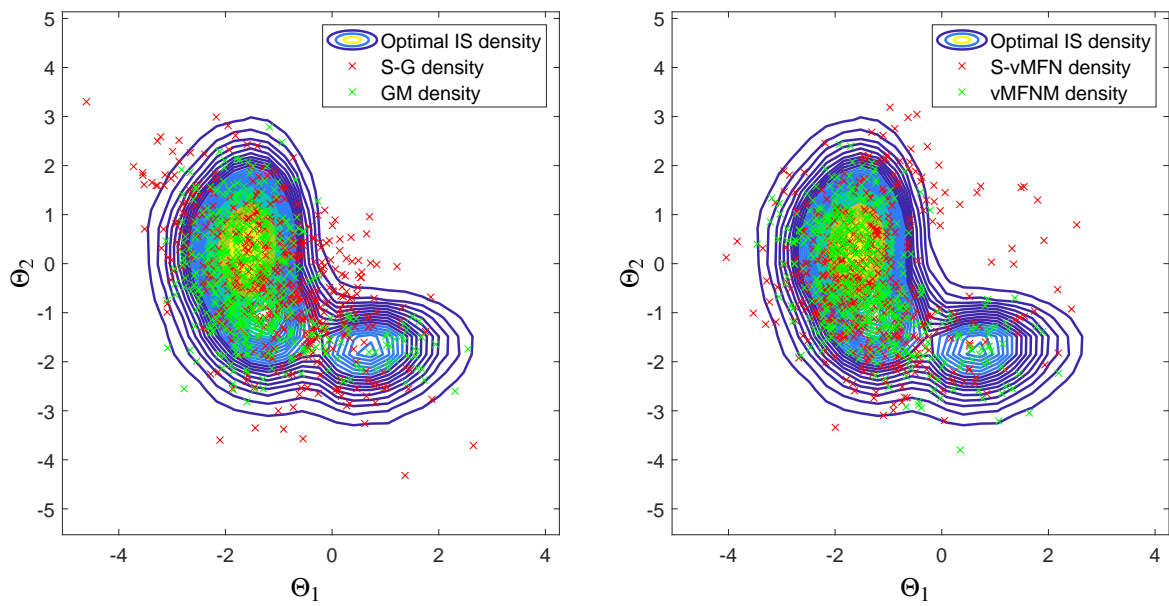


**Fig. 3.** Comparison of the IS density of the uncertain structural parameters in the standard normal space ( $\Theta$ -space) for two-story linear shear frame - case 2. The solid lines represent the contours of the optimal IS density  $h_{\Theta}^*(\theta)$ , which is estimated by direct MCS with  $10^7$  samples. The scattered points are samples of  $\Theta$  drawn from the IS density obtained by the CE-IS method.

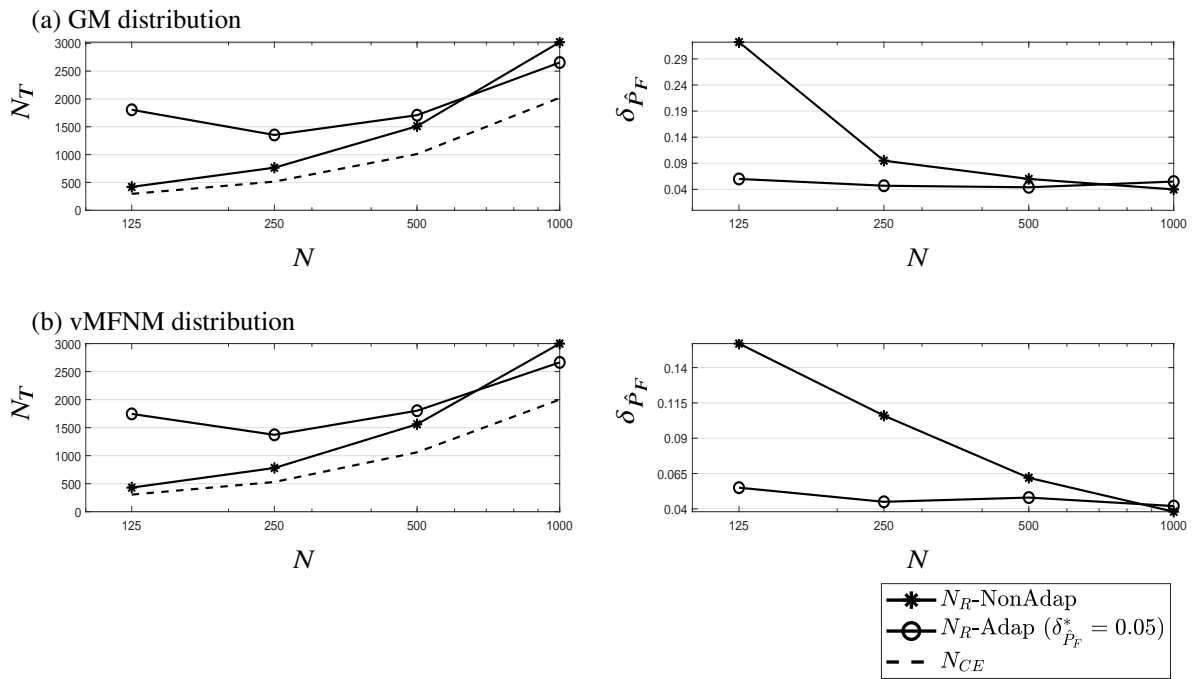


**Fig. 4.** Total computational effort  $N_T$  and the sample CoV  $\delta_{\hat{P}_F}$  as a function of  $N$  for two-story linear shear frame - case 2. The rows correspond to different parametric densities (a) GM distribution; (b) vMFNM distribution. Note that the dashed line does not reflect  $N_T$ , but the computational effort needed only for CE optimization.

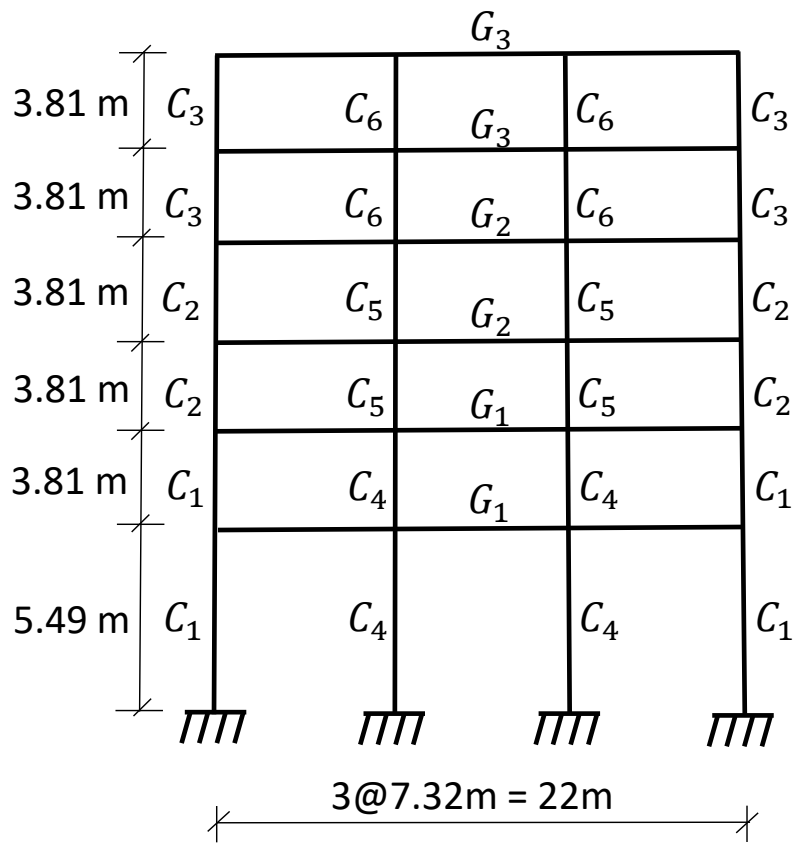


**Fig. 5.** Moment-resisting steel frame